

NASA TECHNICAL NOTE



NASA TN D-5710

C. 1

NASA TN D-5710

LOAN COPY: RETURN TO
AFWL (WLOL)
KIRTLAND AFB, N MEX



EMPIRICAL ANALYSIS OF UNACCELERATED VELOCITY AND MASS DISTRIBUTIONS OF PHOTOGRAPHIC METEORS

by C. D. Miller

Lewis Research Center
Cleveland, Ohio 44135

NATIONAL AERONAUTICS AND SPACE ADMINISTRATION • WASHINGTON, D. C. • MAY 1970



0131522

1. Report No. NASA TN D-5710	2. Government Accession No.	3. Recipient's Catalog No.	
4. Title and Subtitle EMPIRICAL ANALYSIS OF UNACCELERATED VELOCITY AND MASS DISTRIBUTIONS OF PHOTOGRAPHIC METEORS			
7. Author(s) C. D. Miller	5. Report Date May 1970	6. Performing Organization Code	
9. Performing Organization Name and Address Lewis Research Center National Aeronautics and Space Administration Cleveland, Ohio 44135	8. Performing Organization Report No. E-4917	10. Work Unit No. 721-03	
12. Sponsoring Agency Name and Address National Aeronautics and Space Administration Washington, D.C. 20546	11. Contract or Grant No.	13. Type of Report and Period Covered Technical Note	
15. Supplementary Notes	14. Sponsoring Agency Code		
16. Abstract An empirical analysis was performed on data for 2000 sporadic meteors. A bimodal log-normal equation was found for unaccelerated velocity distribution, by empirical curve fitting to match observed velocity distributions for meteoroids within 10 ranges of mass with due regard to failure of observation of faint meteors. An exponent of -1.34 was confirmed in the equation for cumulative influx rate of meteoroids relative to mass. An exponent of -3.87 was established for meteoroid velocity relative to Earth's atmosphere as used in an earlier weighting factor for correction of biasing effects of velocity and mass. Earlier theoretical results were closely approximated.			
17. Key Words (Suggested by Author(s)) Meteors, Meteoroids, Velocity, Mass, Distributions, Photographic, Analysis, Weighting factors	18. Distribution Statement Unclassified - unlimited		
19. Security Classif. (of this report) Unclassified	20. Security Classif. (of this page) Unclassified	21. No. of Pages 56	22. Price * \$3.00

* For sale by the Clearinghouse for Federal Scientific and Technical Information
Springfield, Virginia 22151

CONTENTS

	Page
SUMMARY	1
INTRODUCTION	2
EMPIRICAL EQUATION FOR DISTRIBUTION OF VELOCITY OF METEOROIDS	4
Data to Be Fitted	4
Choice of Tentative Equation Form	6
Theory of mathematical statistics	6
Application of normal distribution to unaccelerated meteoroid velocity data	9
Adjustment of Velocity Distribution to Account for Observational Failure	13
Effect of observational failure on apparent velocity distribution	13
Criterion for discovery of meteors in terms of exposure	14
Normal distribution of observational failure related to photographic density	15
Subdivision of mass ranges for closer approximation of observational failure	19
Fitting of Equation to Data	20
Quality of Fit of Equation to Data	23
EMPIRICAL EQUATION FOR CUMULATIVE MASS DISTRIBUTION	27
EMPIRICAL DERIVATION OF WEIGHTING FACTOR FOR CORRECTION OF PHOTOGRAPHIC BIASES	30
COMPARISON OF EMPIRICAL RESULTS WITH EARLIER THEORETICAL RESULTS	32
BEARING OF RESULTS ON FORMULA FOR LUMINOUS EFFICIENCY	35
CONCLUDING REMARKS	42
APPENDIXES	
A - SYMBOLS	44
B - NORMALIZING FACTOR FOR OFFSET LOG-NORMAL DISTRIBUTION	48
C - STATISTICAL EFFECT OF ZENITH ANGLE AND POSITION OF METEOR WITHIN FIELD OF VIEW	50
D - ERRORS IN EARLIER PUBLICATION ON ANALYSIS OF METEOR DATA	52
REFERENCES	53

EMPIRICAL ANALYSIS OF UNACCELERATED VELOCITY AND MASS DISTRIBUTIONS OF PHOTOGRAPHIC METEORS

by C. D. Miller

Lewis Research Center

SUMMARY

An empirical analysis was performed to estimate unaccelerated velocity (velocity relative to a gravity-free Earth) and mass distributions of sporadic meteoroids. Use was made of data from photographs of more than 2000 meteors, supplied by the Smithsonian Astrophysical Observatory. The observational data used in the empirical analysis were histograms for 10 ranges of meteoroid mass, representing distribution of unaccelerated velocity, which had been weighted only for the focusing effect of Earth's gravity. Use was made of a discovery criterion for meteor traces on photographic plates published earlier, which had been independently derived on both a theoretical and an empirical basis. A normal distribution was assumed to govern the failure of observers to find meteor traces of near marginal density, and this assumption proved to be consistent with the data. An equation for a bimodal log-normal velocity distribution was fitted to the observational data for the 10 mass ranges by a trial-and-error method, and was shown to represent the data nearly as well as would be possible for the size of sample available according to well recognized statistical theory. A weighting factor for simultaneous correction of the velocity and mass biases in the photography of meteors was also deduced on a trial-and-error basis.

Earlier findings reached on a largely theoretical basis were in general only slightly modified. These findings for the photographic range of meteoroid mass included: (1) a value of the exponent of initial velocity of a meteor relative to Earth's atmosphere, contained in a weighting factor to correct for the biasing effects of meteoroid velocity and mass; (2) a histogram obtained with use of the weighting factor for the unaccelerated velocities of meteoroids for all masses, fully corrected except for a statistical bias concerned with direction of meteoroid travel in space; (3) the form of the equation for cumulative mass distribution and the exponent of mass of approximately -1.34 in that equation; and (4) the same velocity distribution for all masses.

The close agreement between the empirical results listed and corresponding earlier theoretical results are thought to provide a substantial support for a considerable quantity of theoretical work done by others which had served as a foundation for the theoretical effort.

INTRODUCTION

Investigators have advanced and studied various criteria, both theoretically and experimentally, for damage to space vehicles by meteoroid impact. Many of those criteria are alike in the fact they contain factors identifiable as meteoroid mass raised to some constant power and impact velocity to the same or some other constant power. The statistical distributions of mass and impact velocity, that is, the frequency of encounter of one mass relative to another and the frequency of occurrence of one velocity relative to another, are important to determine. If they can be established, they can readily be used in conjunction with whatever damage criterion may be selected to estimate the probability of a destructive impact during a specified space mission.

It is particularly desirable to determine the distributions in terms of simple equations. Such equations need not have the mystical property of correctness, or uniqueness as an expression of the distributions. They do not even need to be the most accurate of all equations that could possibly be found. It is only necessary that they conform to the real distributions to a sufficient degree of approximation. It is highly desirable that the equations for mass and velocity distribution be jointly integrable. In that case, a ready calculation can be made of the probability of encounter of a particle that will do critical damage, exceed a critical kinetic energy, exceed a critical momentum, or exceed any critical parameter in terms of powers of mass and impact velocity.

A study of influx rates, masses, and impact velocities of meteoroids was undertaken to obtain an estimate of the hazard to radiators and other components of space vehicles presented by meteoroids in space, that is, by particles like those that produce atmospheric meteors. A further objective for this study was to obtain a more complete knowledge of the nature of the solar system, of which the meteoroids are a part. In this study, use has been made of data obtained from photographs of approximately 2000 sporadic meteors by the Astrophysical Observatory of Smithsonian Institution, which that organization generously provided on punched cards.

Earlier progress was reported in references 1 and 2. Highlights of the progress previously reported were (1) a discovery criterion, or, approximately, a criterion for marginal photographic density of a meteor trace to allow discovery, in terms of powers of meteoroid mass and meteoroid velocity relative to Earth's atmosphere and in terms of other factors of minor importance (ref. 1); (2) a weighting factor developed in reference 1 for adjustment of relative counts of photographic meteors for the photographic biases caused by variations in mass and velocity, which attaches much greater importance to variations in meteoroid velocity relative to Earth's atmosphere than had earlier been thought to exist; (3) a tentative log-normal equation derived to define velocity distribution (ref. 2); and (4) approximate confirmation (ref. 2) of an earlier widely used equation for cumulative mass distribution.

The discovery criterion was developed theoretically (eq. (40) of ref. 1) and was well

confirmed as to its powers of meteoroid mass and velocity on an empirical basis (eq. (45) of ref. 1). Hence, that criterion is believed to be well established. In reference 2, the new weighting factor was confirmed to a substantial degree by correlations produced through its use. However, the validity of the weighting factor, the log-normal equation for velocity distribution, and the equation for cumulative mass distribution all still rested to some extent on a theoretical basis after the work reported in references 1 and 2. It was believed these three results could well benefit from a new independent approach that might obtain the same or better results on a totally empirical basis. Such is the purpose of the work to be reported here, with use from the previous work of only the discovery criterion, which already received its independent empirical confirmation in reference 1.

A valuable by-product of the part of the study reported in references 1 and 2 has been a remarkably accurate confirmation of an integrated body of earlier theoretical work that was used as its foundation. That theoretical work included conclusions by Whipple (ref. 3), Hawkins and Upton (ref. 4), Öpik (ref. 5), Jacchia (refs. 6 and 7), Hawkins and Southworth (ref. 8), and Verniani (ref. 9). Also demonstrated, by the small degree of scatter of statistical results, was the quite adequate accuracy for statistical purposes of the data reduction reported by McCrosky and Posen in reference 10. These results may be the first independent empirical confirmation of this integrated segment of meteor theory. It may be that the further work to be reported now will add more strength to that body of theory.

The first objective in the work now to be reported is the empirical deduction of an equation to fit the observed distributions of unaccelerated velocity of meteoroids within specific ranges of mass. After the data are presented for examination, a brief discussion of necessary theory of mathematical statistics will be presented, including a description of a normal distribution. Next the possibility of extension of the normal distribution to a more general form, necessary to fit the observed data, will be discussed. The influence of observational failure on the more general expression will be considered, with introduction of a criterion for discovery of meteors in terms of photographic exposure and photographic density.

On the foundation described, an equation will be found by trial-and-error variation of various parameters to obtain the best fit possible to the data. An essential part of this effort will involve an estimate of the fraction of all meteors discovered within each mass group. Those fractions will be used, in conjunction with actual counts of meteors within the groups, for an empirical deduction of cumulative mass distribution.

Finally, an empirical deduction of a weighting factor will be performed by trial and error, to operate on all meteors and yield a velocity distribution that agrees with the equation previously found to fit the observed data for the various mass groups.

EMPIRICAL EQUATION FOR DISTRIBUTION OF VELOCITY OF METEOROIDS

A procedure will be described for fitting an analytical equation to observed distributions of unaccelerated meteoroid velocity for various ranges of meteoroid mass by a method as nearly as possible empirical. The observed data will be described, principles of mathematical statistics needed for fitting an equation to the data will be explained, and the actual process of fitting the equation to the data and the results will be disclosed. Symbols used are defined in appendix A.

Data to be Fitted

The empirical data upon which the effort that will be described here was based are shown in figure 1. Each of the 10 parts of that figure is concerned with one of 10 mass ranges or groups (classes of meteoroid mass). The masses were as given by McCrosky and Posen in reference 10. The 10 mass groups of sporadic meteors were the same as those described in reference 2. The number of meteors in each group ranged from 217 in the heaviest group to 172 in the lightest. As described in reference 2, the distribution of velocity v_G , the velocity of the meteoroid relative to the Earth before acceleration by Earth's gravitation, was determined for each of the 10 groups with a weighting factor

$$\varphi_w = \left[1 + \left(\frac{v_e}{v_G} \right)^2 \right]^{-1} \quad (1)$$

in which v_e is the velocity of escape from the Earth's gravitational field, and the factor $\left[1 + (v_e/v_G)^2 \right]^{-1}$ is an approximate adjustment for the focusing effect of Earth gravitation. The derivation of this factor, by various writers, is on too firm and obvious a physical basis to be open to serious question (see ref. 2).

The distributions of v_G so found, with use of the computer program described in reference 2, are shown by the circular symbols in figure 1. The points are plotted just as in figure 3 of reference 2, except that here they are plotted on their observed levels. In reference 2 the points in each plot were shifted vertically for a purpose described there. Obviously the patterns shown by the circular symbols are very different for the different mass groups. The task is now set to find an equation or mathematically definable system governing all these patterns with only minimal help from earlier conclusions.

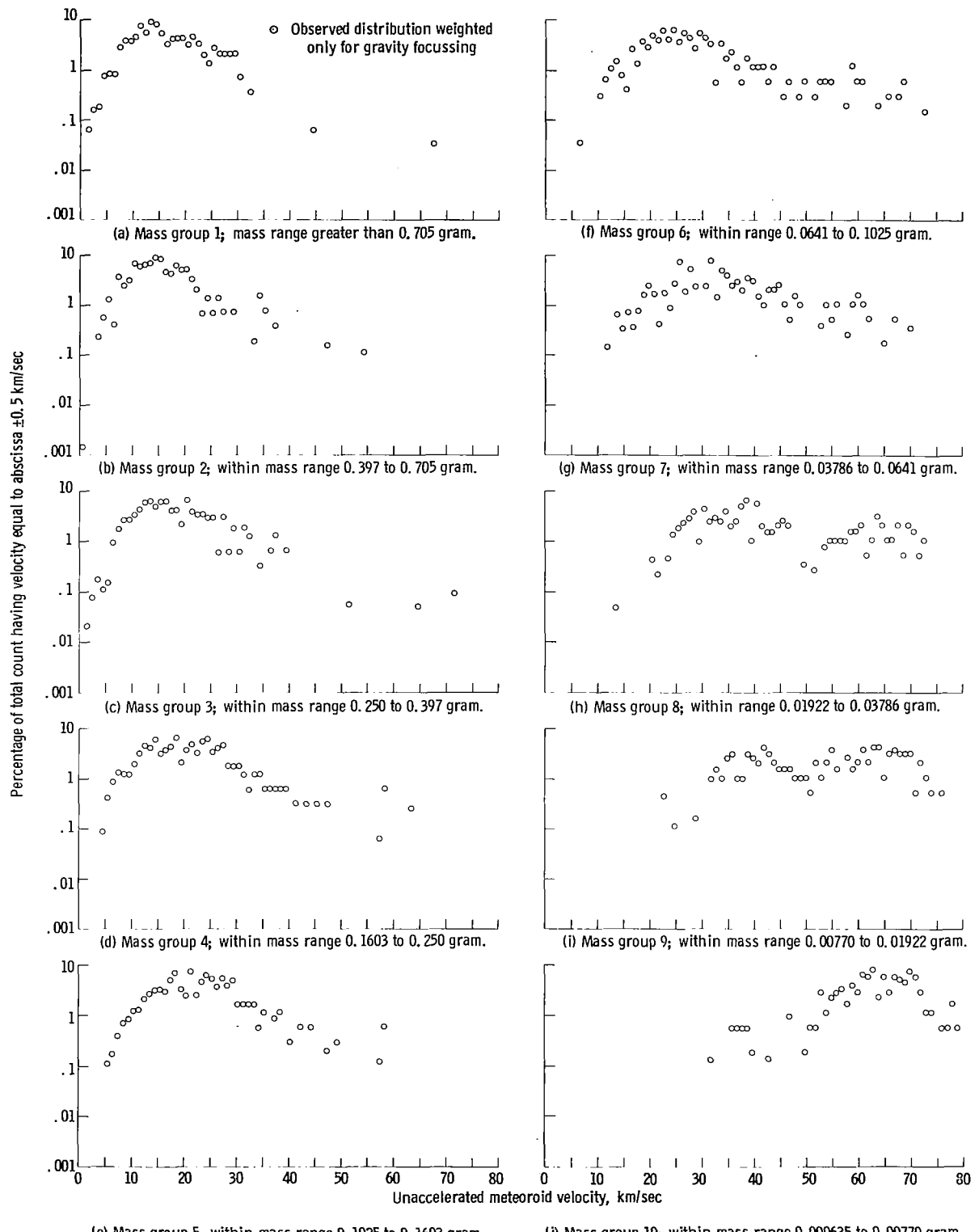


Figure 1. - Observed distribution of velocity relative to gravity-free Earth for sporadic meteors weighted only for gravity focussing.

Choice of Tentative Equation Form

Consideration must first be given to selection of a probable equation form for use. As a preliminary to such choice, some generalized discussion of a few principles of mathematical statistics is desirable.

Theory of mathematical statistics. - A distribution of a random variable is roughly definable as the relative frequencies of occurrence of different values of the variable. This definition sometimes involves immediate confusion because the term "random" is often misunderstood as necessarily implying an equal probability of all values. In fact, however, the term "random" has no real meaning except under the constraint of a specific distribution, either expressed or implied. The cause of the confusion is that often the distribution is rectangular and is not stated but understood. And it is only the rectangular distribution that allows an equal probability of any value within the range of possible values.

Of more widespread real value than the rectangular distribution is the Gaussian, which will be called throughout this paper by its more usual name, the normal distribution. It has such widespread applicability to random variables occurring in nature that its more common name might almost be regarded as descriptive of its general applicability.

The normal distribution of a random variable is expressed by the equation

$$f(x) = a' \exp\left[-\frac{1}{2} \left(\frac{x - \mu}{\sigma}\right)^2\right] \quad (2)$$

where a' , μ , and σ are constants. Here and in other equations expressing statistical distributions, $f(x)$ is to be read as "frequency of x ," which means, approximately, the fraction of all values of the random variable that may be encountered that will have the specified value x within $\pm 1/2$ unit. This function is also known as the probability density of x . This function may be defined by the right-hand side of equation (2) or by other expressions, depending on the type of distribution, whether normal or otherwise.

Now equation (2) is really very restrictive, and it is therefore surprising that it should have such widespread applicability. It appears to contain three arbitrary constants, but in reality it usually has only two, μ and σ . The value of μ is the mean (average) or modal (highest frequency) value. The value of σ is the standard deviation, or a measure of the degree to which a random value tends to depart from the mean. If existence of the random variable within a regime governed by equation (2) is a certainty,

then the total probability for all values of x must equal one, and it is then necessary that

$$a' = \frac{1}{\sqrt{2\pi} \sigma} \quad (3)$$

(see ref. 11 or other text on mathematical statistics). If $p\{E_x\}$ is the probability of the existence of the random variable within the regime governed by equation (2) and is not unity, then the coefficient a' in equation (2) should be replaced by

$$a = p\{E_x\}a' \quad (4)$$

The normal distribution expressed by equation (2) is represented schematically by

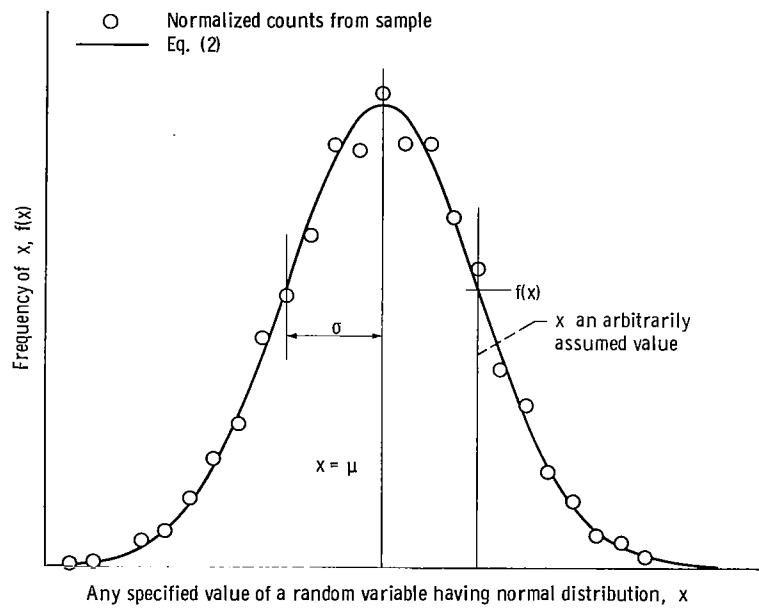


Figure 2. - Schematic representation of normal distribution.

the curve in figure 2. Also shown there are circular symbols such as might be obtained by counting actual cases in which members of a small sample of the random variable have various values x . The larger the sample, the less the tendency for the points to depart from the theoretical curve. By constructing vertical rectangles with upper ends lying on the circular symbols and lower ends at the zero value of the ordinate a "histogram" could be formed.

The theoretical curve represented by equation (2), for a given value of a or a' , has only two degrees of freedom. Changing μ simply moves the curve from side to side without change of shape. Changing σ changes the slimness of the bell shape. But the same effect could be produced with change of scales of abscissa and ordinate, with exactly the same shape of curve.

The area under the curve, as for other types of distribution also, has two properties of interest: (1) The area under the curve to the left of a vertical line representing an arbitrary value of x , divided by the total area under the curve, represents the fraction of all cases within the regime governed by the curve in which the random variable should be expected to have a lower value than x . (2) Any position within the area under the curve selected at random, with an equal probability of choice of any position within the area, has the probability $f(x)$ of having an abscissa value equal to $x \pm 1/2$.

A more accurate definition of the function $f(x)$ is

$$f(x) = p \{ x < V_r < (x + dx) \} / dx \quad (5)$$

where dx has the usual significance of a differential and $p \{ x < V_r < (x + dx) \}$ is the probability that a value of the random variable will lie between x and $x + dx$. It follows, for the normal distribution (eq. (2)) and for the condition $p \{ E_x \} = 1$, that the probability that the random variable V_r has a value less than x must be

$$\begin{aligned} p \{ V_r < x \} &= \int_{-\infty}^x f(t) dt \\ &= a' \int_{-\infty}^x \exp \left[-\frac{1}{2} \left(\frac{t - \mu}{\sigma} \right)^2 \right] dt \end{aligned} \quad (6)$$

which is clearly the area under the curve and to the left of the abscissa x in figure 2. By a change of variable, with

$$\tau = \frac{x - \mu}{\sigma} \quad (7)$$

and with corresponding change in significance of t , equation (6) becomes

$$p \{ V_r < x \} = a' \sigma \int_{-\infty}^{\tau} \exp\left(-\frac{1}{2} t^2\right) dt \quad (8)$$

For τ and x approaching infinity, by equation 586 of reference 12, which reads in effect

$$\frac{1}{\sqrt{2\pi}} \int_{-x}^x \exp\left(-\frac{1}{2} t^2\right) dt = 1 - (2/\pi)^{1/2} \exp\left(-\frac{1}{2} x^2\right) \sum_{i=0}^{\infty} (-1)^i \frac{(2i-1)! x^{-(2i+1)}}{2^{i-1} (i-1)!}$$

equation (8) yields

$$p \{ V_r < +\infty \} = \sqrt{2\pi} a' \sigma \quad (9)$$

As $p \{ V_r < +\infty \}$ is the total area under the curve in figure 2, and must equal $p \{ E_x \}$ of equation (4), equation (9) expresses the same relation as equation (3).

The ordinate of the normal distribution curve of figure 2, or the value of $f(x)$ according to equation (2) is positive and nonzero for all values of x from $-\infty$ to $+\infty$. In cases where a random variable cannot possibly extend throughout such a range, the normal distribution cannot strictly apply. However, in practice, even if the random variable is not normally distributed, often an equation identical in form with equation (2) applies with a suitable change of variable on both sides, or with a suitable change of variable on the right side only.

Because the normal distribution has very wide applicability, equation (2) is a logical choice for initial investigation regarding its possible application to the data plotted in figure 1.

Application of normal distribution to unaccelerated meteoroid velocity data. - Any attempt to apply equation (2) to the distribution of unaccelerated geocentric velocities of meteoroids v_G encounters the immediate difficulty that negative values of v_G are nonexistent. If this velocity were a vector having always the same direction, but with the possibility of opposite senses, then a meaning would exist for a negative value. But v_G is just the scalar value of a vector that has many directions in space.

An immediate obvious recourse is to substitute $\ln v_G$ for x , on the right side of equation (2), and v_G for x on the left side, giving the log-normal equation

$$f(v_G) = a' \exp \left[-\frac{1}{2} \left(\frac{\ln v_G - \mu}{\sigma} \right)^2 \right] \quad (10)$$

(A more usual form of equation (10) would replace a' with a'/v_G . The constants a' and μ then have different values and μ has a different physical significance. Equation (10) is more suitable for use here, and it represents the same log-normal distribution.) A schematic representation of this distribution appears as the solid-line curve in figure 3, which is obviously skewed in comparison with the normal distribution of figure 2.

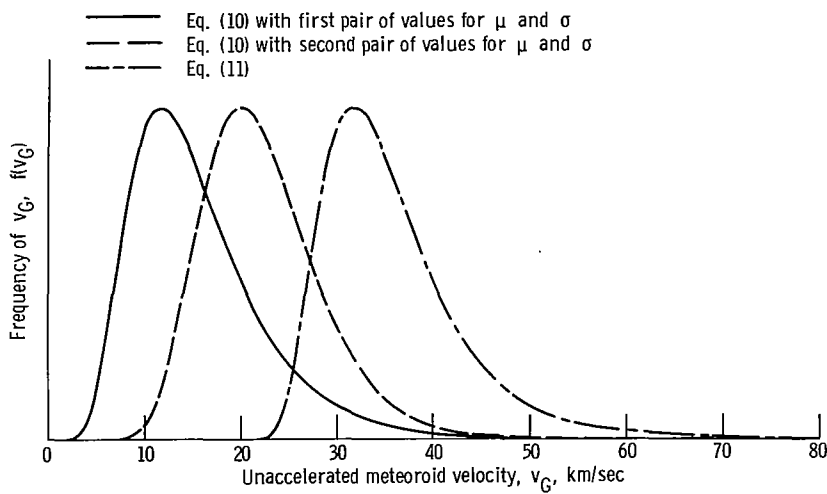


Figure 3. - Schematic representations of three log-normal distributions.

ure 2. The dashed line in figure 3 is also a schematic representation of equation (10), but with different values of μ and σ designed to shift the curve to the right while retaining the same modal (peak) value. But a change in shape has occurred. The dashed-line curve is more nearly symmetrical.

The dash-dot line in figure 3, however, does have the same shape and the same modal value as the solid-line curve and is shifted far to the right. This result, which could be accomplished for the ordinary normal distribution by simply changing the value of μ , is obtained now by introducing a new constant δ to produce an offset log-normal equation,

$$f(v_G) = a' \exp \left\{ -\frac{1}{2} \left[\frac{\ln(v_G + \delta) - \mu}{\sigma} \right]^2 \right\} \quad (11)$$

in which a change in value of δ shifts the curve bodily from right to left without other change. Of course, equation (10) is only a special case of equation (11).

It is shown in appendix B that for $p\{E_x\} = 1$ the coefficient a' in equation (10) or (11) must be

$$a' = \frac{1}{\sqrt{2\pi} \sigma \exp\left(\mu + \frac{1}{2}\sigma^2\right)} \quad (12)$$

within sufficient approximation for all cases in which we shall be concerned here. Thus, under this condition, equation (11) has three arbitrary constants instead of two and is thus less restrictive than equation (2).

The reason for the presence of the new constant is that it specifies the extent to which the range of the random variable is restricted. For example, with $\delta = 0$, the permissible range is $0 < v_G < \infty$, while with δ approaching ∞ the range of permissible values of the random variable is $-\infty < v_G < \infty$, the same as for equation (2). In fact, if δ is made large without limit, and suitable scales of ordinate and abscissa are used, the curve of figure 2 can be duplicated within any given range within any specified degree of accuracy by equation (11). Hence, it is seen that equation (11) is more general than either equation (2) or (10) and virtually includes both of them. It therefore has greater capacity to fit various empirical distributions.

Now if any one of the log-normal curves of figure 3 is compared with the plotted data points on figure 1(a), with due allowance for the fact the scale of figure 1 is semi-logarithmic while that for figure 3 is linear, some hope seems to exist that an approximate fit would be possible. However, in parts (d) to (i) of figure 1, one modal value clearly will not do. The probability density in the neighborhood from $v_G = 45$ to $v_G = 50$ is lower than either above or below this range. This condition may even be true in all 10 parts of figure 1, but not evident in the earlier parts of the figure because of paucity of data above $v_G = 50$ in parts (a) to (c).

But a second modal value can easily be provided by simultaneous use of two equations having the form of equation (11), one for the lower velocity regime, the other for the higher velocities. It is of no consequence whether the two regimes can be identified with any physical conditions. Also, though the regimes overlap, there is no need to identify any meteoroid count as belonging to one regime or the other.

With subscript 1 for the low velocity and subscript 2 for the high velocity regime, the unknown values of $p\{E_x\}_1$ and $p\{E_x\}_2$ can be interrelated by a single unknown parameter R with the equations

$$p\{E_x\}_1 = \frac{1}{R + 1} \quad (13)$$

and

$$p\{E_x\}_2 = \frac{R}{R+1} \quad (14)$$

Obviously the necessary condition is met that

$$p\{E_x\}_1 + p\{E_x\}_2 = 1 \quad (15)$$

Now, from equations (4), (11), (13), (14), and (15), a single expression may be written for a combination of the two regimes as

$$f(v_G) = \left(\frac{1}{R+1}\right) a'_1 \exp\left\{-\frac{1}{2}\left[\frac{\ln(v_G + \delta_1) - \mu_1}{\sigma_1}\right]^2\right\} + \left(\frac{R}{R+1}\right) a'_2 \exp\left\{-\frac{1}{2}\left[\frac{\ln(v_G + \delta_2) - \mu_2}{\sigma_2}\right]^2\right\} \quad (16)$$

This equation is integrable, numerically when not integrable formally, and if it can be fitted to the data with suitable values of the constants it will be of substantial analytical value. It has seven independent constants that may be varied for the purpose of fitting to plotted data, namely, μ_1 , σ_1 , μ_2 , σ_2 , δ_1 , δ_2 , and R . The constants a'_1 and a'_2 are defined in terms of independent constants by equation (12).

The solid-line curve of figure 4 is a schematic representation of equation (16). The dashed-line is the same curve as it might be modified by failure to observe slow-moving meteors. Variation of the parameter R varies the ratio of the two modal values, that is, the ordinates of the two peaks. Variation of μ_1 and μ_2 shifts the abscissas for the modes, with a concomitant increase of symmetry as a mode is shifted toward the

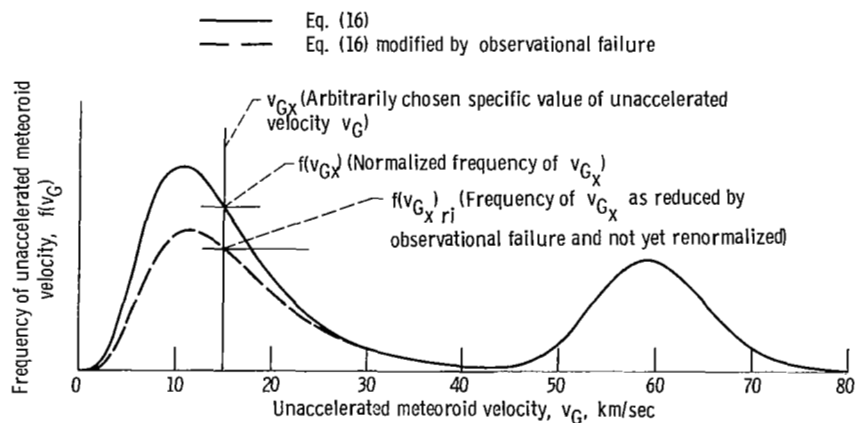


Figure 4. - Schematic representation of effect of observational failure on bimodal log-normal distribution of unaccelerated meteoroid velocity.

right. Variation of σ_1 and σ_2 changes the slimness of the humps. Variation of δ_1 and δ_2 shifts the positions of the humps sidewise.

With these rather considerable resources available for varying the shapes of the curves in figure 4, we may now begin to see some hope of fitting at least some of the data in all 10 parts of figure 1. In attempting to do so, we may begin with the simplest assumption that the velocity distributions for all the mass groups are actually the same and that the apparent differences as seen in the different parts of figure 1 are due to failure of observation as shown by the dashed line of figure 4. Such procedure is in accord with the principle that the simplest explanation of data should be assumed until some reason is found to depart from it. Failure of observation at lower velocities unquestionably occurs, and it occurs more severely with lower masses than with higher masses. It is only reasonable to assume that heavier particles and faster particles will produce meteors that are more easily photographed. Hence, before we make any serious attempt to fit equation (16) to the data in all parts of figure 1, we need to study the relation between the solid curve and the dashed curve in figure 4.

Adjustment of Velocity Distribution to Account for Observational Failure

The actual shape of a curve such as the dashed-line curve of figure 4, to account for observational failure, may be determined. For this and other incidental purposes, some detailed consideration will now be given to the nature of the observational failure.

Effect of observational failure on apparent velocity distribution. - It is obvious at once, if the existing conditions can be represented properly by curves such as those of figure 4, that the fraction of particles within a mass group i that are discovered on the photographic plates is

$$F_i = A_r \quad (17)$$

where A_r is the total area under the dashed curve, because the area under the solid curve is unity. (The dashed curve is asymptotic with the solid curve, but for convenience is shown as identical with it everywhere to the right of the point where they join.) Also, if the dashed curve is to match the data points in any of the 10 parts of figure 1, all its ordinates must be divided by F_i for the purpose of normalization, that is, making the value $p\{E_x\} = 1$ for the dashed curve. This operation is necessary because the empirical distributions represented by the data points in figure 1 were normalized.

Now consider that the solid curve of figure 4 is basically applicable to all 10 mass groups and that the dashed curve applies specifically to a mass group i . Consider any arbitrarily chosen velocity v_{G_x} within the region in which some observational failure

occurs. Let $f(v_{G_x})$ represent the frequency of v_{G_x} according to equation (16), and let $f(v_{G_x})_{ri}$ represent the reduced frequency of v_{G_x} for mass group i (unnormalized), that is, the apparent frequency, reduced by observational failure. Now a ratio defined as

$$F_{i(v_{G_x})} = \frac{f(v_{G_x})_{ri}}{f(v_{G_x})} \quad (18)$$

and hence any similar ratio for any velocity v_G , that is,

$$F_{i(v_G)} = \frac{f(v_G)_{ri}}{f(v_G)} \quad (19)$$

may be readily computed under the assumption that observational failure is normally distributed relative to photographic density of the meteor trace, that is, to the degree of darkening of the photographic emulsion. Such an assumption is reasonable. Observational failure is a form of human error, an inevitable random variation in the performance of any observer in searching the photographic plates for meteor trails. A normal distribution of errors is so usual that a common name for an integral of equation (2) is "the error function."

Photographic density is related to the optical parameter known as exposure. Before photographic density may be related directly to observational failure as represented by equations (18) and (19), some consideration needs to be given to the problem of a critical exposure level, or discovery criterion.

Criterion for discovery of meteors in terms of exposure. - In evaluating the ratio $F_{i(v_{G_x})}$ we will need a criterion with which the likelihood of discovery of a meteor may be judged (eq. (46) of ref. 1) which reads as follows

$$C_{marg} = m_{\infty}^{1.02} v_{\infty}^{2.93} (\cos Z_R)^{0.167} F(Z_R)_{av}^{-0.54} \quad (20)$$

where m_{∞} is the mass of a meteoroid before any ablation by passage through Earth's atmosphere, v_{∞} is the velocity of the meteoroid relative to Earth's atmosphere before the atmosphere has imposed any decelerating effect, Z_R is the angle of meteor path to the zenith, and $F(Z_R)_{av}$ is a statistically expected value of a function of Z_R and the

position of the meteor within the fields of view of the cameras, as described in reference 1. The significance of the discovery criterion C_{marg} is that, at least roughly, if and only if it exceeds some unknown critical value, the trace of the meteor can be discovered in examination of the photographic plates.

The discovery criterion C_{marg} of equation (20) was derived theoretically, and the exponent of v_∞ was confirmed almost exactly on an empirical basis in reference 1. The exponent in equation (20) is the one that was determined empirically. Appendix C shows that the factors $(\cos Z_R)^{0.167}$ and $F(Z_R)^{-0.54}$ are unimportant statistically relative to the purpose for which C_{marg} will be used here. They cannot be used in the method that is to be followed here, and will therefore be omitted. Elimination of v_∞ , however, is neither necessary nor desirable. The abscissa v_G in each part of figure 1 is a function of v_∞ , since v_∞ always exceeds v_G approximately by an amount caused by addition of kinetic energy to the meteoroid equal to the energy of escape from Earth's gravitational field. Because of the empirical determination in reference 1 of the pertinent parts of equation (20), use of the discovery criterion C_{marg} involves no departure from the aim in this paper to confirm or modify the important results of references 1 and 2 on a basis as nearly as possible empirical.

With omission of the unusable factors, equation (20) becomes

$$C_{marg} = m_\infty^{1.02} v_\infty^{2.93} \quad (21)$$

The comparison of theoretical with empirical results in reference 1 indicated that C_{marg} is very nearly a critical value of effective photographic exposure. In the procedure to be used here it must be treated as such. Unquestionably the differences in photographic density must be the principal factor governing success in discovery of meteor trails, and photographic density is related to exposure by well known laws. Hence, no great departure from empiricism is involved in the treatment of C_{marg} as an effective exposure.

To make use of this assumption regarding the criterion C_{marg} , it is now necessary to review a small amount of well established photographic theory regarding density.

Normal distribution of observational failure related to photographic density. - The density of a uniformly darkened area on a developed emulsion is defined (see ref. 13 or other photographic handbook or textbook) as the logarithm to the base 10 of a ratio equal to a quantity of light incident upon the emulsion divided by the quantity of that light transmitted by the emulsion. The densities that would be involved here would be only slightly above threshold levels. For such densities, the following equation applies at least approximately,

$$D = \gamma \log E + D_0 \quad (22)$$

where D is density, E is exposure or the integrated product of the intensity of illumination that caused the darkening of the developed emulsion by the duration of the time interval throughout which the illumination existed, and D_0 and γ , constants, are characteristics of the emulsion and the conditions of its development. For very faint densities, corresponding to the 'toe' of the characteristic curve, the rate of increase of density with exposure is somewhat less than indicated by equation (22); that is, the local value of γ gradually increases toward a constant value. However, reduction of the photographs as reported in reference 10 depended upon the ability to see a meteor trace through two emulsions simultaneously. This condition would eliminate much of the toe of the characteristic curve.

The criterion C_{marg} of equation (21) approximates an exposure in undefined units. That is, from equations (21) and (22),

$$D = \gamma \log \left(C_1 m_{\infty}^{1.02} v_{\infty}^{2.93} \right) + D_0 \quad (23)$$

where C_1 is an unknown constant. Or

$$D = \gamma \log C_1 + \gamma \log \left(m_{\infty}^{1.02} v_{\infty}^{2.93} \right) + D_0 \quad (24)$$

For the purpose of this analysis the values of the constants γ , $\log C_1$, and D_0 are inconsequential, as will be seen later. Hence, for simplicity, equation (24) may be re-written as

$$D = \log \left(m_{\infty}^{1.02} v_{\infty}^{2.93} \right) \quad (25)$$

As v_{∞} can be derived from v_G by addition of kinetic energy equal to the energy of escape at Earth's surface, equation (25) may be converted to

$$D = \log \left[m_{\infty}^{1.02} \left(v_G^2 + v_e^2 \right)^{1.465} \right] \quad (26)$$

For use in equation (26), the square of the velocity of escape was taken as

$$v_e^2 = \frac{2g r_s^2}{(r_s + h_{av})} = 123.25 \text{ km}^2/\text{sec}^2 \quad (27)$$

in which g is the acceleration due to gravity at Earth surface (taken as 9.81×10^{-3} km/sec²), r_s is the radius of the Earth (in kilometers) at Earth surface at the camera sites (taken as 6368), and h_{av} is the average height of the meteors (in kilometers) above ground level (taken as 90).

Now, to apply the assumption of a normal distribution of observational failure, regard D of equation (26) as the abscissa in figure 2. Regard the abscissa value μ in that figure as μ_d , an unknown critical value of D at which one-half the pertinent meteors will be discovered in examination of the photographic plates. Regard the distance σ in the figure, in the direction of the axis of abscissas, as σ_d , an inverse measure of the sharpness of cutoff of observational failure in the neighborhood of μ_d . Regard the abscissa value x in the figure as an arbitrarily chosen value of D , that is, as D_x . Then, equation (2), represented by figure 2, becomes

$$f(D_x) = a' \exp \left[-\frac{1}{2} \left(\frac{D_x - \mu_d}{\sigma_d} \right)^2 \right] \quad (28)$$

equation (3) becomes

$$a' = \frac{1}{\sqrt{2\pi} \sigma_d} \quad (29)$$

and with $p\{E_x\} = 1$, because every meteoroid will produce a theoretically calculable density and hence will fall within the regime of equation (28), equation (28) becomes

$$f(D_x) = \frac{1}{\sqrt{2\pi} \sigma_d} \exp \left[-\frac{1}{2} \left(\frac{D_x - \mu_d}{\sigma_d} \right)^2 \right] \quad (30)$$

To this point, adaptation of figure 2 and equation (2) to the concept of observational success in relation to photographic density has been easy. Less facile is the matter of assigning a physical significance to $f(D_x)$ of equations (28) and (30). Such significance must be expressed if confidence is to exist in application of the normal distribution to this problem.

For this purpose, consider for the moment two fictitious conditions: (1) while a searcher is examining a photographic plate, each meteor trace slowly and gradually increases in density from negative infinity until it reaches the density at which it is discovered by the searcher; (2) the searching history, that is, the time interval during which the plate has been under examination and during which the trace densities have been increasing, is unrelated to the discovery of traces. Otherwise expressed, condition (2) is that discovery or failure to discover a trace of a given density depends only on such things as the concentration and the pattern of star images in the vicinity of the trace, accidental dark spots, blemishes, and so forth.

Under these two conditions, $f(D_x)$ may be defined as

$$f(D_x) = \frac{p\{D_x < D_d < (D_x + dD)\}}{dD} \quad (31)$$

where dD , as before, is a differential, D_d is the density at which a particular trace is discovered, and $p\{D_x < D_d < (D_x + dD)\}$ is the probability that a particular trace will be discovered after it has reached the density D_x and before it has reached the density $(D_x + dD)$. It is then obvious that, of all traces that have reached the density D_x , the fraction discovered will be the area under the curve in figure 2 to the left of the abscissa value D_x .

Now in the real case, condition (2) of the fictitious case is unnecessary because the history of gradual increase in density, the effect of which condition (2) was intended to eliminate, does not exist. With the assumption in both the fictitious and the real case that the searcher did the best he could, the fraction of meteor traces with density D_x that he discovers in both cases should be the same. That is, such fraction will be

$$\begin{aligned} F(D_x) &= \frac{1}{\sqrt{2\pi} \sigma_d} \int_{-\infty}^{\tau_x} \exp\left(-\frac{1}{2} t^2\right) dt \\ &= 0.5 + \frac{\tau_x}{\sqrt{2\pi}} \sum_{i=0}^{\infty} (-1)^i \times \frac{\tau_x^{2i}}{2^i i! (2i+1)} \end{aligned} \quad (32)$$

where

$$\tau_x = \frac{D_x - \mu_d}{\sigma_d} \quad (33)$$

(See ref. 11 or other textbook on mathematical statistics and reference 12 or other table of integrals.) The values of the three constants dropped between equations (24) and (25) would affect the values of μ_d and σ_d , but not the values of τ_x or $F(D_x)$. Hence, elimination of the three constants of unknown value was justified.

Now if the mass range for mass group i were infinitely narrow, so that any meteoroid within the range would have a definite mass m_i , then a density $D_{x(i)}$ could be calculated with substitution of m_i for m_∞ and v_{G_x} for v_G in equation (26), the result could be substituted for D_x in equations (32) and (33), and then $F(D_x)$ from equation (32) would be the desired value $F_{i(v_{G_x})}$ as defined in equation (18). For the real

condition, with a substantial range of values of m_∞ within a mass group, a close approximation to the value of $F_i(v_{G_x})$ may be reached by dividing the range into a large number of subranges.

Subdivision of mass ranges for closer approximation of observational failure. - An approximation of $F_i(v_{G_x})$ for mass range i may be obtained by subdividing mass group i into a large number of subranges. Then, for the velocity v_{G_x} , the median mass $m_{m(j)}$ of each subrange j may be used as described for mass m_i above to determine a value $F(D_{x_j})$, corresponding to the value $F(D_x)$ obtainable with use of m_i . An average of all the values $F(D_{x_j})$ then gives a close approximation of the desired fraction $F_i(v_{G_x})$ of equation (18). That is,

$$F_i(v_{G_x}) = \frac{1}{n} \sum_{j=0}^n F(D_{x_j}) \quad (34)$$

where n is the number of subranges used, provided the subranges have been so chosen that each should contain the same expected number of meteoroids. Finally, with use of $F_i(v_{G_x})$ from equation (34), the value of $f(v_{G_x})_{ri}$ as shown in figure 4 may be determined with equation (18), using a value of $f(v_{G_x})$ determined with equation (16); that is,

$$f(v_{G_x})_{ri} = f(v_{G_x}) F_i(v_{G_x}) \quad (35)$$

Thus a complete dashed-line curve as in figure 4 may be generated as a series of specific values of $f(v_{G_x})_{ri}$ for each mass group i , for $i = 1$ to $i = 10$. It is only necessary to know the values of the constants μ_d and σ_d and to find a way to subdivide a mass range i into subranges all having the same expected content.

For the subdivision, the frequently used equation form for cumulative mass influx rate (ref. 4)

$$F_{>m} = \alpha m^{-\beta} \quad (36)$$

is available, in which m is any mass that might be specified, $F_{>m}$ is the influx rate of particles of mass greater than m , and α and β are constants. At this point, use of this equation is a departure from the aim of empiricism. However, it may not necessarily be permanently so. A confirmation, or replacement of, equation (36) is one of the desired end results of the present paper. Perhaps a large error in the form of equa-

tion (36), or in an assumed value of the exponent $\beta = 1.34$, at this point, will have small effect on the end result, so that substitution of the end result for equation (36) would permit an iteration of the entire procedure that would converge to constant empirical form of the equation and value of β . That possibility will be further considered after the end result is obtained.

From inspection of equation (36), equal increments of $F_{>m}$ must occur for equal increments of $m^{-\beta}$. Hence, a mass group with range extending from m_{\min} to m_{\max} may be subdivided into n subranges of mass, with each expected to include the same influx rate of meteoroids, by specifying minimum and maximum values of m_{∞} for subrange j , for $j = 1$ to $j = n$, as

$$m_{\min(j)} = \left[m_{\min}^{-\beta} + \frac{(j-1)(m_{\max}^{-\beta} - m_{\min}^{-\beta})}{n} \right]^{-1/\beta} \quad (37)$$

$$m_{\max(j)} = \left[m_{\min}^{-\beta} + \frac{j(m_{\max}^{-\beta} - m_{\min}^{-\beta})}{n} \right]^{-1/\beta} \quad (38)$$

Then the median value of m_{∞} for subrange j must be

$$m_m(j) = \left\{ m_{\min(j)}^{-\beta} + \frac{1}{2} \left[m_{\max(j)}^{-\beta} - m_{\min(j)}^{-\beta} \right] \right\}^{-1/\beta} \quad (39)$$

Fitting of Equation to Data

Now, with an assumed value $\beta = 1.34$, we are ready to attempt to fit curves like the dashed curve of figure 4 to the plotted data in all parts of figure 1, with a single equation (16) including a single set of values for all the constants in that equation, and with the method that has just been described for providing the expected change in shape of the observed distribution curve because of failure of observation at the lower velocities for the different mass groups. In this attempt, we have extensive capability for adjusting the shapes of the curves by selection of the proper values of $\mu_1, \sigma_1, \delta_1, \mu_2, \sigma_2, \delta_2, R, \mu_d$, and σ_d . The expected effects of changes in the values of the first seven of these parameters have already been discussed. Now, with reference to figure 4, increase in the value of μ_d should be expected to drive the point where the dashed curve closely approaches the solid curve farther to the right. Increase in the value of σ_d should be expected to decrease the rate at which the curves diverge from each other as we proceed

toward the left from that point. It must be remembered, of course, that all the values of $f(v_{G_x})_{ri}$ calculated with equation (35) must be divided by F_i of equation (17), which may be approximately evaluated as

$$F_i = \sum_{k=1}^{80} f(k - 0.5)_{ri} \quad (40)$$

in which $(k - 0.5)$ is a value of v_{G_x} as used in equation (35) and in which the upper limit of summation is 80 because no values of v_G higher than 80 appear in the plotted data. On semilogarithmic plots this normalization simply raises the level of each value of $f(v_G)_{ri}$ by the same amount, with no consequent change in shape of the curve represented by the values of $f(v_G)_{ri}$.

Figure 5 shows the end result of the curve fitting effort that has been described. The triangular plotted points represent the normalized calculated values of $f(v_G)_{ri}$. The solid-line curves were simply ruled through the triangular symbols. In each part of the figure, they represent equation (16) as modified by observational failure. The dashed-line curves represent roughly a distance of one standard deviation above the solid-line curves as will be discussed. The value of n , the number of subranges used within each mass group, was 100.

The substantial degree of success in fitting the curves to the data for all mass groups as seen in figure 5 was achieved by trial and error, with independent variation of the nine parameters R , δ_1 , δ_2 , μ_1 , μ_2 , σ_1 , and σ_2 of equation (16), and μ_d and σ_d of equation (33). The data points taken from figure 1, the calculated and normalized values of $f(v_G)_{ri}$, and the solid-line curves were automatically plotted by the computer for a given set of assumed values of the nine parameters. The results were examined, a new set of the nine parameters was chosen by visual judgment of the quality of fit, and the procedure was repeated. The effects of variation of the individual parameters were clear cut and not readily confused. The results shown in the figure were obtained with the values of seven of the varied parameters as they appear in or are implied ($\delta_1 = \delta_2 = 0$) by the equation

$$f(v_G) = 0.0736 \exp\left[-\frac{1}{2}\left(\frac{\ln v_G - 2.37}{0.455}\right)^2\right] + 3.036 \times 10^{-4} \exp\left[-\frac{1}{2}\left(\frac{\ln v_G - 4.078}{0.09657}\right)^2\right] \quad (41)$$

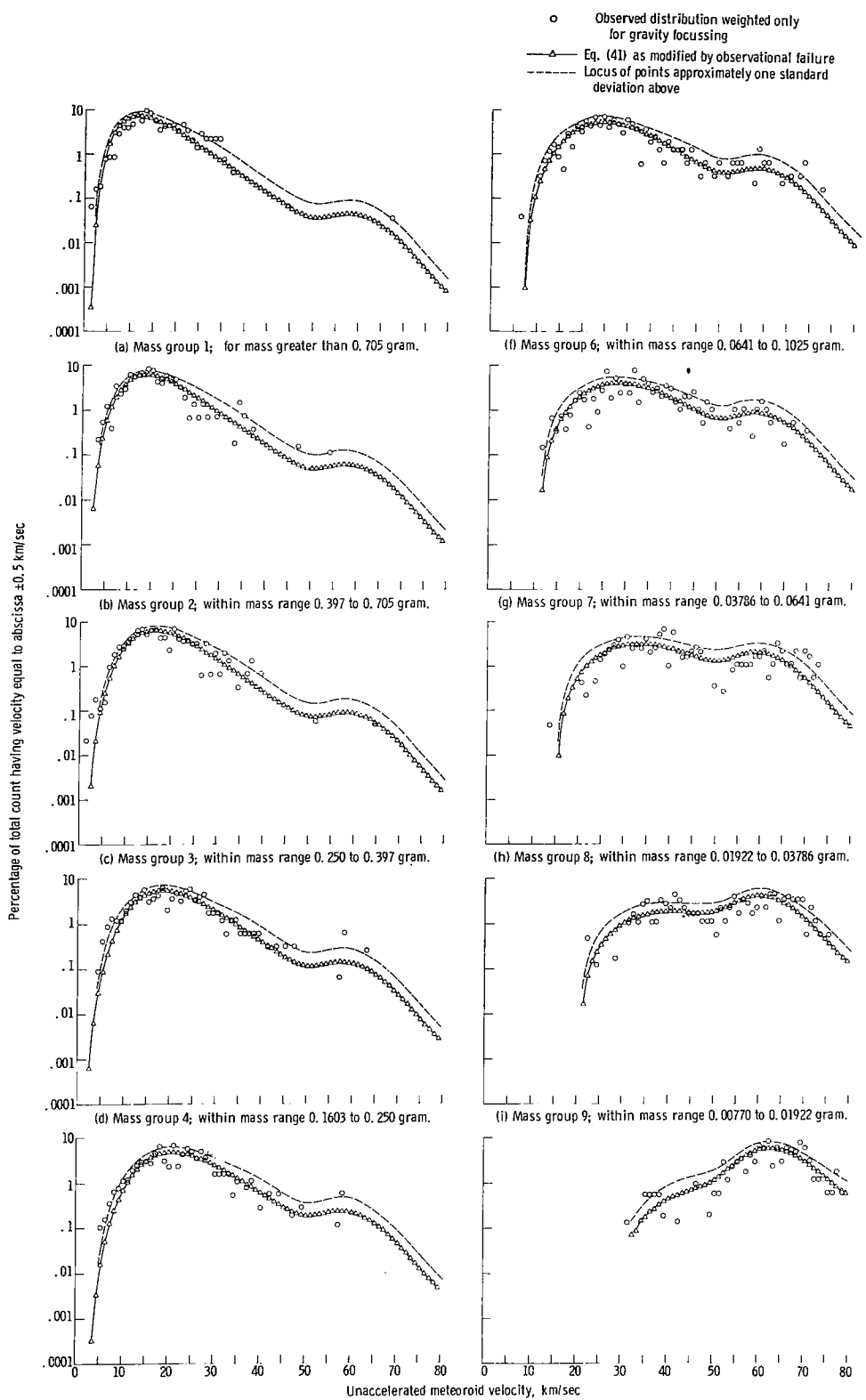


Figure 5. - Fit of equation to observed distribution of velocity relative to gravity-free Earth for sporadic meteors weighted only for gravitational focussing.

and with

$$\left. \begin{array}{l} \mu_d = 3.25 \\ \sigma_d = 0.32 \end{array} \right\} \quad (42)$$

Quality of Fit of Equation to Data

The method of judging quality of fit of equation (41) to the data in figure 5 that will now be described is unrelated to the procedure used in the actual fitting of the data. That procedure was solely by visual judgment as to how well the solid-line curves represented the trend of the plotted symbols, and without regard to the dashed-line curves, which were not even constructed on the plots during that fitting procedure. The purpose here is rather to appraise the quality of the fits finally achieved.

Superficially, of course, the best possible fit of curves to the data would require curves that passed through all data points. However, by well known statistical principles, if the probable accuracy of individual plotted points is finite and calculable, no true "best" fit actually exists. Instead, if fitted curves pass well established tests with a sufficiently high score, then those curves may theoretically be considered as good a fit to the data as any other curves could be although not necessarily better.

In judging the quality of fit of the solid-line curves in figure 5, it should be appreciated that each circular symbol represents only a small number of meteors, almost always less than 20 and in many cases only one or two. Substantial scatter of the data should therefore be expected. In particular, in parts (a) to (c) of figure 5, for the lowest velocities the levels of the plotted circular symbols should be given no weight. Dr. R. E. McCrosky, one of the authors of reference 10, has indicated privately that the values of v_∞ reported in that reference were accurate only within a few percent. The determinations of values of v_∞ were primary, and the determinations of v_G were derived from them. Hence, at the lowest velocities, the frequencies shown by the plotted points should be expected to be too high because of error.

For example, a value of v_G equal to 0.5 kilometers per second would correspond to a value of v_∞ equal to 11.102, while a value of v_G equal to 3.5 would correspond to a value of v_∞ equal to 11.14. The difference in v_∞ is less than 0.4 percent. In figure 5(a), the level of the solid-line curve at $v_G = 3.5$ ($v_\infty = 11.14$) calls for discovery of approximately one meteor in the total sample. For $v_G = 0.5$ ($v_\infty = 11.102$) it

calls for perhaps 0.0001 meteor. Now if the one observed meteor that should be expected to occur at $v_\infty = 11.14$ is determined erroneously to have a velocity $v_\infty = 11.102$, then the circular symbol in the figure for $v_G = 0.5$ would appear far too high because of that one error alone. No possible compensating errors could bring it down. This same condition will exist in the relation between any two low values of v_G , as long as the correct distribution curve (the solid-line curves in figure 5) is ascending very steeply. The condition only gradually disappears as (1) an integer difference in value of v_G approaches a large percentage difference in value of v_∞ and (2) the distribution curve ascends less steeply. Errors of this type are virtually certain to occur. Hence, falsely high frequencies should be expected at these low values of v_G . For this reason, in the discussion that follows, the positions of data points for values of v_G less than 3.5 kilometers per second will be ignored in all 10 parts of figure 5.

The quality of the fit in any of the charts may be judged by the ratio between (1) the total number of the circular symbols between the solid curve and the dashed-line curve and (2) the total number of symbols above the solid-line curve. The background will now be explained for construction of the dashed-line curves.

For the normal distribution represented in figure 2, 68.27 percent of the values of a random variable will lie within one standard deviation of the mean value (see ref. 11 or other textbook on mathematical statistics). However, the ordinate for any circular symbol on any of the 10 parts of figure 5 is not governed by a normal distribution. The ordinate is proportional to the number of meteors actually discovered within the mass and velocity ranges indicated (adjusted for the effect of gravity focusing). As already explained, the levels of the triangular points in the figures were computed under assumption of observational failure governed by a normal distribution relative to photographic density. Presumably the levels of the circular symbols have been affected in the same manner. But in addition to the calculated statistical effect of observational failure, an inevitable irregularity in time of arrival of meteors exists. The calculated observational failure acts as a kind of screen, which reduces the average rate of arrival of meteors in a particular range of mass and a particular range of velocity. But the chronological variation of actual occurrence of meteors exists both before and after the screening effect. It is governed not by a normal distribution but by the Poisson distribution. Thus, if the solid-line curve in figure 5(a) indicated, for example, that μ meteors should have been discovered at a particular velocity $v_G \pm 0.5$ kilometer per second, in spite of the observational failure, then obviously not exactly μ meteors would have been found unless μ were an integer. This fact would be true even if the solid-line curve were absolutely correct. The probability of discovery of any particular integral number

of meteors x (where x can equal μ only if μ is an integer) would be

$$\varphi(x) = \frac{\mu^x \exp(-\mu)}{x!} \quad (43)$$

(see ref. 11 or other textbook on mathematical statistics). The value of μ would have been higher if observational failure did not occur, but equation (43) still applies with the reduced value of μ .

In general, even if the distribution is not normal, it is expected that approximately 68 percent of the data points will lie within one standard deviation of the mean. In this case, however, to avoid any doubt on the subject, the dashed-line curves in figure 5 were determined in a somewhat different manner, which will be described with reference to figure 6. The circular symbols in that figure represent the values of $\varphi(x)$ according to equation (43) for integral values of x , with an arbitrarily chosen value of $\mu = 3.5$. The function, of course, is undefined for nonintegral values of x . The standard deviation σ is shown, only approximately in its correct position.

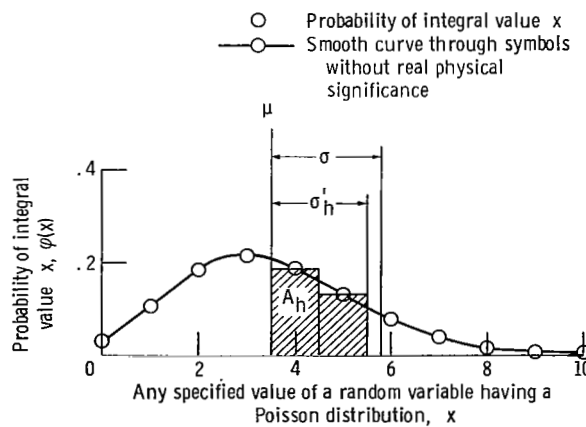


Figure 6. - Poisson distribution for mean value of 3.5.
 $(\mu$, mean value; σ , standard deviation on high side of μ ; σ'_h , approximate equivalent standard deviation; A_h , area equal to 68.27 percent of total area under smooth curve on high side of mean value.)

An approximate equivalent standard deviation σ'_h is shown, applicable to the high side of μ only, which is designed to represent more nearly the distance on the high side of μ within which 68.27 percent of the data points should lie. The distance σ'_h is determined by (1) passing a smooth curve through the circular symbols and (2) constructing a vertical line by trial and error at an abscissa value $\mu + \sigma'_h$ such that the shaded area A_h will be 68.27 percent of the total area under the curve to the right of the abscissa value μ .

Now σ'_h , so determined, will have a strict physical interpretation only when μ and σ'_h each happen to have a value equal to an integer plus one half, as they appear in figure 6. Then the area A_h would be approximated by the sum of the areas of the rectangles of unit width constructed with their upper ends through the circular symbols, and actually 68.27 percent of the values greater than μ would really lie between the values μ and $\mu + \sigma'_h$.

The logarithm of $(\mu + \sigma'_h)/\mu$ in general represents the distance between the solid-line curves and the dashed-line curves in figure 5. For example, in figure 5(a) the level of the solid-line curve at $v_G = 11.5$ kilometers per second was estimated to call for actual discovery of $\mu = 18$ meteors. The value of σ'_h was determined by the method described as 4.45, and $\log[(\mu + \sigma'_h)/\mu]$ was therefore 0.096. The dashed-line curve, accordingly, was constructed as nearly as possible at a distance of 0.096 above the solid-line curve at the value of $v_G = 11.5$ kilometers per second in figure 5(a).

Now, in that same example, because nonintegral numbers of meteors are not possible, two physically meaningful limits might be set, one greater, the other lower than $\log[(\mu + \sigma'_h)/\mu]$. The lower might really call for perhaps a 58.5 percent probability and the higher for perhaps a 70 percent probability that the data point, if on the high side of μ , would be included. The corresponding probability for any distance between those two limits would be the same as for the lower limit, because no actual data point could lie between the two limits.

The method of construction of the dashed-line curves, therefore, provided that at all points on each chart the curve would lie between the closest limit that would include less and the closest limit that would include more than 68.27 percent of the data points on the high side. The average effect of such distances for all positions on the charts should be closely 68.27 percent.

In construction of the curves, a value of μ less than unity was never used because, in effect, in velocity ranges in which occurrence of meteors was very sparse the velocity intervals were increased roughly to correspond to a probable occurrence of one meteor.

Construction of dashed-line curves below the solid-line curves in the figures by an analogous process was considered. The problem was complicated by the fact the logarithm of zero meteors within a velocity interval is negative infinity, could not be plotted,

TABLE I. - INDICATION OF QUALITY OF FIT
 OF CURVES TO DATA FOR OBSERVED
 DISTRIBUTION OF UNACCELERATED
 VELOCITY FOR METEORS OF
 VARIOUS MASS GROUPS

Figure	Percentage of data points within theoretical 68.27 percent limit
5(a)	56.8
5(b)	50.0
5(c)	67.5
5(d)	56.3
5(e)	60.8
5(f)	84.7
5(g)	69.3
5(h)	57.2
5(i)	50.0
5(j)	57.8

and had to be ignored. Because of this complication, and because the single dashed-line curve is sufficient for the purpose, no dashed-line curves were constructed below the solid-line curves.

Above 2.5 kilometers per second, the percentage of data points between the curves, relative to the total above the solid-line curve, is as shown in table I. The percentage for all the mass groups as a whole was 62.5 percent, within 5.77 percent of the theoretical optimum. If only 1.2 data points for each mass group were shifted from a position above the dashed line to a position between the two lines, the fit of the curves would be the theoretical optimum. That is, other curves could be theoretically as good but not better. The indication, then, is that a substantially more meaningful fit to the data would not be possible without a larger sample, or that equation (41) is nearly as accurate as would be theoretically possible to determine with the available data.

EMPIRICAL EQUATION FOR CUMULATIVE MASS DISTRIBUTION

A fallout of the work that has been described is the easy empirical determination of cumulative mass distribution as shown in figure 7, with use of the values of F_i of equation (40).

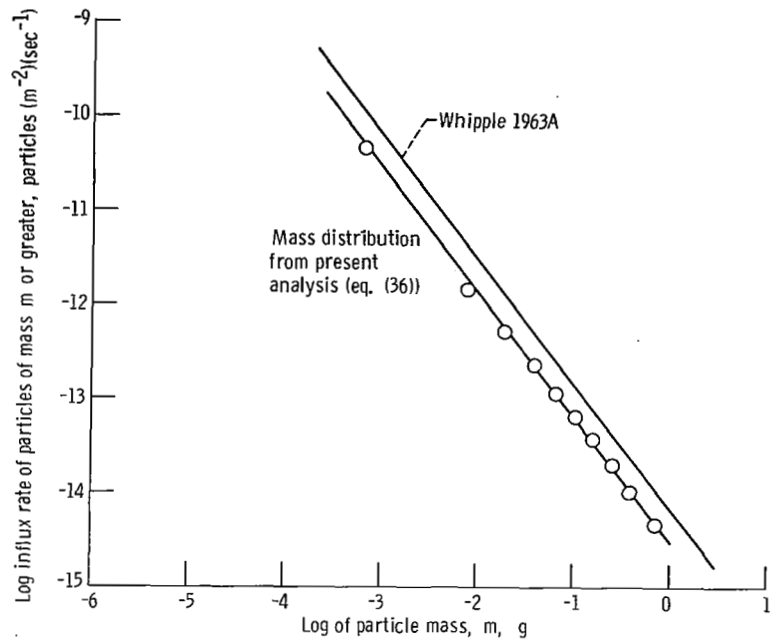


Figure 7. - Distribution of influx rate of meteors relative to mass, with adjustment for gravitational focussing.

TABLE II. - COMPUTATIONS FOR DETERMINATION OF INFLUX
DISTRIBUTION OF METEOROIDS RELATIVE TO MASS -
ADJUSTED FOR GRAVITY FOCUSING

Mass group	Fraction of particles discovered (F_i of eq. (40))	Count uncorrected except for gravity focusing	Fully corrected count, particles $m^{-2} \text{ sec}^{-1}$	Fully corrected cumulative count, $F_{>m}$, particles $m^{-2} \text{ sec}^{-1}$	Lower mass limit, g
1	8.657×10^{-1}	132.1	4.55×10^{-15}	4.55×10^{-15}	7.05×10^{-1}
2	5.921	109.8	5.53	1.008×10^{-14}	3.97
3	4.017	129.6	9.62	1.97	2.50
4	2.565	145.5	1.692×10^{-14}	3.66	1.603
5	1.514	132.4	2.608	6.27	1.025
6	8.158×10^{-2}	133.2	4.869	1.114×10^{-13}	6.41×10^{-2}
7	3.896	152.6	1.168×10^{-13}	2.28	3.786
8	1.518	139.2	2.734	5.02	1.922
9	4.202×10^{-3}	132.8	9.42	1.444×10^{-12}	7.70×10^{-3}
10	8.231×10^{-5}	119.7	4.336×10^{-11}	4.48×10^{-11}	6.35×10^{-4}

The data used in determining the cumulative mass distribution appear in table II. The second column shows the values of F_i for each of the 10 mass groups, that is, for $i = 1$ to $i = 10$. Column three shows the count of meteors in each mass group, weighted according to equation (1) to correct, approximately, the effect of gravity focusing. The values in column four are quotients of the values in columns three and two, multiplied by a factor 2.982×10^{-17} to convert to particles per square meter per second. The source of that factor depends essentially on acceptance of a basic value from equation (16) of reference 4 in a manner explained in reference 2. (Nothing has been done in this work or in refs. 1 or 2 to determine the vertical level of the line in fig. 7 independently, but only to determine its slope.) As F_i of column two is the computed fraction of all meteors within the range of mass group i that should have been discovered, division of the count of meteors actually discovered in mass group i (column three) by F_i should yield the total number of incident meteors within the mass group including those that could not be discovered.

Column five of table II shows on line i the total of the values in column four from line one to line i . Column six shows the lower mass limit of each group for use in plotting the points in figure 7. Thus, the values in column five of table II plotted relative to the values in column six should show the cumulative mass distribution according to equation (36), from which the values of α and β may be deduced.

Such a plot of the values in columns five and six of table II appears on a full logarithmic scale in figure 7. (As was explained in ref. 2, the mass values given in ref. 10 have been adjusted upward by a factor of 6.4.) The plotted points show a slope of -1.34. The slope is the same as for the Whipple 1963A line as also shown in figure 7 (ref. 3). The higher level for the Whipple 1963A line is due to the correction for the gravity focusing effect. The level of the straight line in figure 7, representing the 10 plotted points, corresponds to a value of α in equation (36) equal to $10^{-14.525}$.

Further consideration may now be given to the earlier mentioned departure from the aim of empiricism in the use of equation (36), with a value $\beta = 1.34$, in the writing of equations (37) to (39). As a test of the effect of such use of equation (36), the computer program that produced the results shown in figure 5 and in the second column of table II was rerun with use of equation (41) and a value of β in equations (37) to (39) equal to 1.00, and again with β equal to 1.67. Significant differences were not encountered either in the appearance of figure 5 or in the values of F_i in column two of table II. Hence, the assumption of the value of $\beta = 1.34$ did not cause that value to be shown by figure 7.

Even the form of equation (36) is confirmed by figure 7 because a different form of the equation would, in effect, call for varying slopes within the different line segments joining the plotted points. Drastic changes of assumed slopes to $\beta = 1.00$ and $\beta = 1.67$ for all the line segments should have had the same effects on the 10 individual parts of

figure 5 and the individual values of F_i as if those changes of assumed slope had been made for individual mass groups only.

Hence, it is clear that any assumed cumulative mass distribution instead of equation (36) would have allowed rapid convergence to equation (36) upon iteration of the work that has been reported. It follows that use of equation (36) no longer represents any departure from empiricism.

EMPIRICAL DERIVATION OF WEIGHTING FACTOR FOR CORRECTION OF PHOTOGRAPHIC BIASES

Equation (41) representing the statistical distribution of velocity v_G for meteoroids of all masses may now be used for empirical determination of a weighting factor φ_w for correction of photographic biases.

Parameters that can cause a variation in photographic effectiveness are the velocity v_∞ , particle mass m_∞ , zenith angle Z_R , position of meteor within the field of view of the cameras, particle density, particle shape, and possibly particle spin. For a sample as large as 2000, it seems reasonable to expect that the three last named parameters will not show a systematic effect relative to v_G or m_∞ , and they will be ignored.

Now the desired weighting factor φ_w should be usable in the following manner: (1) all sporadic meteors of all mass groups will be examined in series without regard to mass, (2) each meteor will be counted as φ_w meteors rather than as one meteor; (3) total counts of φ_w will be obtained for each velocity interval of one kilometer per second; (4) the totals of item (3) will be converted to percentages of the grand total count of values of φ_w ; (5) a histogram will be constructed from the results of item (4); and (6) the resulting histogram should agree as closely as possible with equation (41).

A weighting factor theoretically obtained in reference 1 (eq. (75) of that ref.) included factors $(\cos Z_R)^{-0.196}$ and $F(Z_R)_{av}^{0.730}$. These factors were based in part on an equation reproduced as equation (20) of the present paper. As already mentioned, appendix C shows that these factors are of small statistical importance. They were not used previously in this paper because: (1) they were shown to be unimportant and (2) they could not be used. In the work now to be reported, however, they can and will be included as part of the weighting factor φ_w . To do so does not involve a departure from the aim of empiricism, because the purpose in this paper is to examine the interrelations of v_G and m_∞ as empirically as possible. At the same time, it is desired that the weighting factor found should be the best possible and should therefore include the results of previous work that are not affected by the empirical purpose here. The desired weighting factor should, of course, also include the adjustment for gravitational

focusing, the right-hand side of equation (1).

Now, in accordance with usual practice for an unknown function, we might well try an assumed expression

$$\varphi_w = m_\infty^\nu v_\infty^\xi (\cos Z_R)^{-0.196} F(Z_R)_{av}^{0.730} \left[1 + \left(\frac{v_e}{v_G} \right)^2 \right]^{-1} \quad (44)$$

and seek definite numerical values for the exponents ν and ξ .

The search for a satisfactory combination of values of ν and ξ may be aided by a good first guess for either value, even though that guess may be only intuitive. The purpose of the factor φ_w is to obtain a distribution of v_G independent of mass m_∞ . It has already been shown that the observed distributions for various mass groups are well explained on the assumption (eq. (41)) of a single distribution of v_G for all masses. Giving a nonzero value to ν in equation (44) would suggest that the velocity distribution to be found is dependent on m_∞ after all. Hence, as a first try in a trial-and-error empirical determination of values of ν and ξ , a zero value for ν seems sensible.

So, in attempting to verify this first choice for ν and to determine the unknown value of ξ , it is only necessary to obtain adjusted distributions for the entire sample of

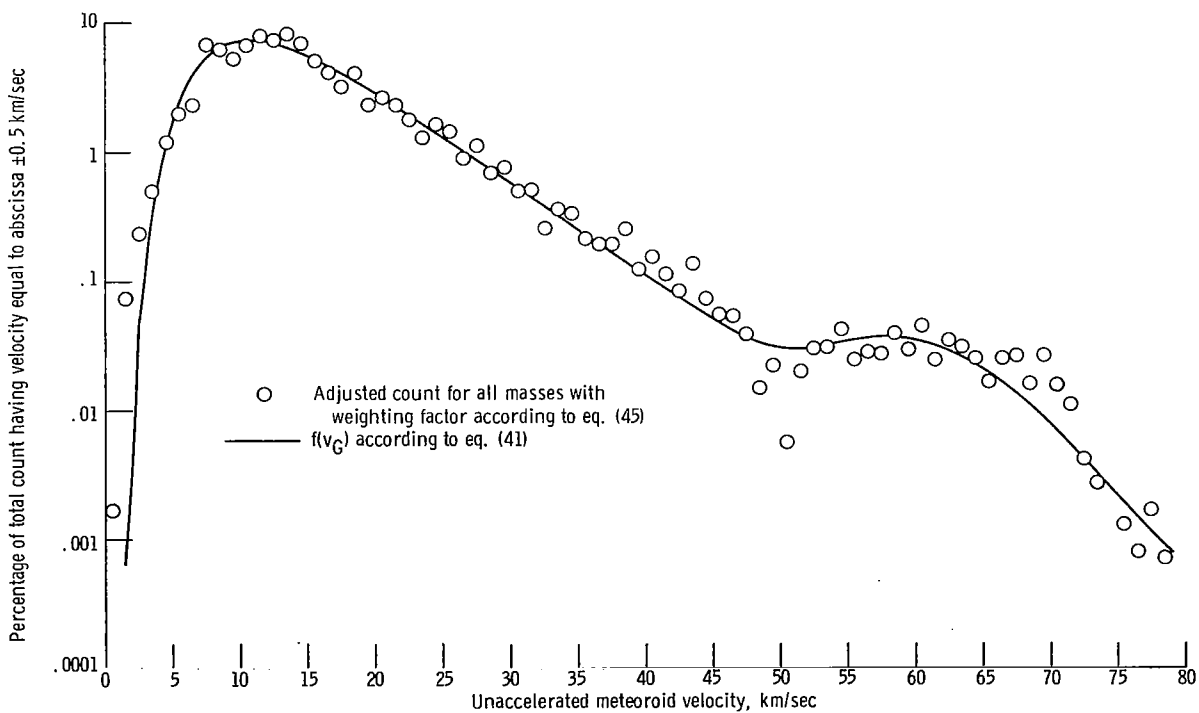


Figure 8. - Velocity distribution of sporadic meteors relative to gravity-free Earth weighted as velocity relative to atmosphere to -3.87 power.

sporadic meteors, using the six-item procedure that has been described, and using one value of ξ after another until item (6) is satisfied. Figure 8, in which the curve represents equation (41) and in which the ordinates of the circular symbols depend upon the value of ξ , shows the end result of this procedure with $\nu = 0$ and $\xi = -3.87$. The corresponding expression of the weighting factor used for the results shown in figure 8 is

$$\varphi_w = v_\infty^{-3.87} (\cos Z_R)^{-0.196} F(Z_R)_{av}^{0.730} \left[1 + \left(\frac{v_e}{v_G} \right)^2 \right]^{-1} \quad (45)$$

The result would be only slightly different with the factor

$$\varphi_w = v_\infty^{-3.87} \left[1 + \left(\frac{v_e}{v_G} \right)^2 \right]^{-1} \quad (46)$$

As discussed earlier relative to figure 5, the plotted data points for the lowest values of v_G should be expected to lie above the true distribution curve.

COMPARISON OF EMPIRICAL RESULTS WITH EARLIER THEORETICAL RESULTS

Almost totally empirical results have now been obtained as follows: (1) a bimodal log-normal expression for distribution of meteoroid velocity v_G independently of particle mass (eq. (41)), (2) values of μ_d and σ_d (eq. (42)) for use in equation (30) governing failure of discovery of meteors on the basis of photographic density as expressed by equation (25), (3) a cumulative influx distribution relative to mass m_∞ (eq. (36)), (4) exponents for m_∞ and v_∞ in a weighting factor for correction of photographic biases (eq. (46)), and (5) a corrected histogram representing true distribution of velocity v_G independently of mass m_∞ (fig. 8).

Assumptions involved were (1) a normal distribution of failure to discover meteors on the basis of photographic density, (2) independence of velocity distribution and mass distribution, (3) the applicability of equation (36), and (4) the form of equation (44) for the weighting factor φ_w . Use of equation (21) for photographic exposure was an adaptation of empirical results from reference 1.

Assumption (3) was removed from the category of an assumption by the clear indication that any other assumption would have lead to the same result by an iterative process. Assumptions (1), (2), and (4) now have the empirical support that at least the data are adequately explained on the basis of those assumptions.

Now let us compare the empirical results described with the earlier theoretical re-

sults from references 1 and 2. Although those results will be referred to hereinafter as theoretical, they actually were partly empirical in the facts that they depended on equation (21) (see ref. 1) and that they included a demonstrated approximate agreement between a theoretically adjusted velocity distribution and portions of observed distributions for 10 mass groups (see ref. 2).

In reference 2, no attempt was made to fit a bimodal equation to a theoretically adjusted histogram for v_G , as could well have been done. However, the best fit possible was found for an offset log-normal equation, with values of constants as they appear in the following equation:

$$f(v_G) = 0.070 \exp \left\{ -\frac{1}{2} \left[\frac{\ln(v_G + 1.5) - 2.46}{0.44} \right]^2 \right\} \quad (47)$$

This equation representing a theoretically weighted histogram in reference 2 differs only slightly from the part of empirically derived equation (41) that refers to the lower velocity regime, which is by far the dominant one of the two regimes.

The value $\beta = 1.34$ for use in equation (36), obtained from the empirically derived figure 7, is identical with the value obtained from the theoretically derived figure 5 of reference 2. The form of equation (36) was confirmed by both the empirical and theoretical figures. The value $\alpha = 10^{-14.525}$ particles per square meter per second, as derived from figure 5, compares with a value $\alpha = 10^{-14.63}$ found in reference 2. The small difference is due to the necessity (in ref. 2) to assume no failure of observation in the two heaviest mass groups.

The only important difference between the theoretically and empirically derived figures is that in figure 5 of reference 2 the plotted points for mass groups 9 and 10 fell far below the straight line representing the other points. They did so for an obvious reason that was explained in reference 2. But the method used there provided no means of calculating their correct levels and confirming that they should fall on the same straight line as the other eight points, as has been done here.

Hence, the important effect of the empirical result here is to increase confidence in the theoretically derived value of β and to extend the range of confidence down through the minimum values of m_∞ within the photographic range.

The empirical finding that the exponent of m_∞ in the weighting factor (ν in eq. (44)) is equal to zero agrees exactly with the theoretically derived weighting factor φ_w of equation (75) of reference 1. The empirical finding of an exponent -3.87 for v_∞ in equation (45) (ξ of eq. (44)) compares with a value of -4.22 in equation (75) of reference 1. The empirically determined value -3.87 is believed to stand on a firmer basis than the value -4.22 from reference 1. However, the difference is slight in effect. A

construction of a figure with use of $\xi = -4.22$ (not presented herein) was but little different from figure 8.

Use of the value 3.87, it will be remembered, was necessary to provide the curve fit shown in figure 8 with use of equation (41). Equation (41) was needed to provide the curve fits of figure 5. The most likely source of the slight discrepancy seems to be uncertainties involved in the treatment of the effect of altitude on area of camera field of view in reference 1. As indicated in that reference, those uncertainties left the exponent of v_∞ undetermined except that it should be within the range from -3.85 to -4.22. The factor $v_\infty^{2.93}$ in the expression for C_{marg} in equation (46) of reference 1 was based on empirical results fully as dependable as the results shown in figure 5. Moreover, it was close to the theoretically derived factor $v_\infty^{2.842}$ in equation (40) of reference 1. Also, the factor $v_\infty^{2.93}$ appears in equation (25) and was therefore used in the determination of the curves in figure 5.

Equation (60) in reference 1 was an expression for φ_{cor} , which was equivalent to φ_w of equation (75) of that reference, but without an adjustment for the larger field of view of the cameras at greater heights of the meteors. That equation followed mathematically from: (1) equation (46) with the factor $v_\infty^{2.93}$; (2) the relation $F_> = \alpha m^{-1.34}$; and (3) the assumption of the same distribution of v_G for all masses. The results shown in figure 5 either support each of these three items independently or are based upon them. Hence, the results here support the factor $v_\infty^{-3.85}$ in equation (60) of reference 1 even independently of the empirical use of the nearly identical factor $v_\infty^{-3.87}$ in obtaining the results plotted in figure 8. The exponent in the empirically deduced factor $v_\infty^{-3.87}$ differs from the value in equation (60) of reference 1 by only about one-half percent.

The conclusion appears necessary that the transformation in reference 1 between equations (60) and (75) must be rejected. That transformation involved only a correction for the effect of meteor altitude upon area of the field of view. Several imponderable considerations were neglected. The work of reference 10 involved superposition of photographs having annular fields of view. Those fields of view coincided best at a particular altitude. Hence at least part of the theoretical increase in area at a higher altitude was nullified by the reduced coincidence of the two fields. Also, as mentioned in reference 1, a specific difficulty existed in discovery of low-speed meteors not associated with their effective exposures. As this difficulty was associated with speed of image on emulsion rather than linear speed of meteor in the sky, it would become worse for a meteor of the same linear speed at higher altitudes and would thus tend to offset the advantage of a larger field of view. Another offsetting factor might be a possible limitation on discovery of a meteor based on the total length of its trace.

The evidence of the present work seems to call for rejection of equation (75) of reference 1 and a firm acceptance of an equation almost identical with equation (60) of that reference, rewritten in the form

$$\varphi_w = (\cos Z_R)^{-0.22} F(Z_R)_{av}^{0.712} v_\infty^{-3.87} \quad (48)$$

All exponents in equation (48) are greater than in equation (60) of reference 1 in the ratio 3.87/3.85.

As may be deduced from appendix C, equation (48) might well be reduced to

$$\varphi_w = v_\infty^{-3.87} \quad (49)$$

for use with a large sample, which, with addition of the factor to correct for gravitational focusing, becomes equation (46).

The best that can be said for the factors $(\cos Z_R)^{-0.22}$ and $F(Z_R)_{av}^{0.712}$ is that their desirability is indicated by the work of reference 1 and that they have not since been shown to be deleterious. On the other hand, the factor $v_\infty^{-3.87}$ in equations (48) and (49) now seems to be well supported.

BEARING OF RESULTS ON FORMULA FOR LUMINOUS EFFICIENCY

A critical question in meteor physics during recent years has been that of a correct formulation for luminous efficiency. It is believed the results of this analysis, in conjunction with recently published work by Dalton (ref. 14) throw some important new light on this subject.

Luminous efficiency was treated in references 1 and 10 as being linearly related to particle velocity and independent of particle mass, as first indicated by Öpik (ref. 5). Öpik substantially revised this formulation for luminous efficiency (ref. 15), disturbing both the linear relation to velocity and the independence of mass. Any error in the formulation used by McCrosky and Posen (ref. 10) for luminous efficiency would of course cause errors in their mass determinations. The finding, both here and in reference 2, that the velocity distribution is independent of mass consequently comes into question, as well as the validity of figure 7 and equation (36) and their counterparts in reference 2.

No attempt will be made here to relate the many statistical studies by other authors to the question. Many such studies needed the weighting factor of equation (48) or, in the simpler approximate form, equation (49), which was not available when those studies were made. The treatment here will deal only with the bearing of the present study on the matter of luminous efficiency in conjunction with reference 14. Although this author disagrees with Dalton's conclusion in favor of Öpik's formulation as presented in reference 15, he finds great value in certain parts of Dalton's paper as will become apparent in the following discussion.

Unlike the earlier parts of this paper, this discussion will presume that the reader has copies of references 1 and 2 at hand, as well as reference 14. Otherwise, considerable unnecessary reproduction of earlier figures and discussions would be necessary.

The formulation for luminous efficiency presented by Öpik in reference 15 is complex and not convenient for formal combination with other mathematical expressions in which the luminous efficiency might be one argument of a function along with other parameters. However, one manner in which it can be represented as a generalized function for direct application to photographic data is as follows:

$$\tau_L = \tau_0 v_\infty^k \epsilon(m_\infty, v_\infty) \quad (50)$$

where τ_0 and k are constants and $\epsilon(m_\infty, v_\infty)$ is a function of m_∞ , v_∞ , and possibly other parameters, that does not contain any constant nonzero power of v_∞ as a factor independently of m_∞ . The linear relation of luminous efficiency τ_L to velocity v_∞ as proposed earlier by Öpik and as used in this study is, of course, the same as the relation expressed by equation (50) with both k and $\epsilon(m_\infty, v_\infty)$ equal to unity.

A valuable part of Dalton's recent work in reference 14 was an approximate confirmation by an independent method of the finding both here and in reference 2 that the velocity distribution is independent of the McCrosky and Posen masses (see for example the almost zero linear correlation between his m_A (the McCrosky and Posen mass) and the air-entry velocity v_∞ for subsample A below the diagonal in his fig. 16). Although zero linear correlation does not absolutely confirm statistical independence, statistical independence does imply zero linear correlation. Hence the near-zero correlation by Dalton tends to make the statistical independence appear plausible.

If k in equation (50) had a value other than unity, with $\epsilon(m_\infty, v_\infty)$ assumed equal to one, the masses used here and in reference 10 would have to be multiplied by v_∞^{1-k} . Superficially it would appear that the mass could no longer be statistically independent of velocity. This question was discussed in appendix F of reference 2. In that discussion the symbol m_∞ was used to designate the masses of reference 10. The symbol m'_∞ was used to designate those same masses multiplied by v_∞^{1-k} , that is,

$$m'_\infty = m_\infty v_\infty^{1-k} \quad (51)$$

Now obviously the relation between m'_∞ and m_∞ as shown by equation (51) involves v_∞ . But this fact does not mean that m'_∞ is basically a function of v_∞ without any regard to m_∞ . It was shown in appendix F of reference 2 that, if v_∞ is statistically independent of m_∞ and if the cumulative distribution of m_∞ is correctly expressed by equation (36), then (1) v_∞ must also be statistically independent of m'_∞ , and (2) the

cumulative distribution of m'_∞ must also be expressed by equation (36) with the same value of β .

In review of appendix F of reference 2, the author has discovered errors as detailed in appendix D of this report. However, those errors do not affect the two conclusions that have just been enumerated. The statement of the nature of the errors seems to imply a dependence of mass on velocity v_∞ , but only superficially so.

The basic purpose of the power of v_∞ in the weighting factor φ_w is to convert from a lower cutoff limit of m'_∞ in the McCrosky and Posen sample to the lower cutoff limit m_∞ . If in equation (51) $k = -1.93$, then, approximately,

$$m'_\infty = C_{\text{marg}} \quad (52)$$

in accordance with equation (21). In that case, the lower cutoff limit in the McCrosky and Posen sample would be m'_∞ and the raw distribution of velocity existing in the sample, after correction for $\cos Z_R$, $F(Z_R)_{\text{av}}$, and for gravitational focusing, would be the true distribution without any need of the power of v_∞ in the weighting factor. It would be so regardless of the actual value of m'_∞ , that is, the actual value of C_{marg} , at which observational cutoff occurred. The need for conversion from a lower cutoff limit of m'_∞ to a lower cutoff limit of m_∞ is precisely to comply with the conclusion stated in appendix F of reference 2, "the ratio of influx rates at any two velocities is different with m'_∞ constant than with m_∞ constant, but nevertheless unchanging from one constant value of m_∞ to another." The symbols m_∞ and m'_∞ could be interchanged in that conclusion.

Some additional insight on this matter may be gained by reflection regarding equation (36) and figure 7. Mutual statistical independence of m_∞ and v_∞ permits writing

$$F_{>m}(v_G) = \alpha_{v_G} m^{-\beta} \quad (53)$$

and

$$\alpha = \int_0^\infty \alpha_{v_G} dv_G \quad (54)$$

where $F_{>m}(v_G)$ is the same as $F_{>m}$, but restricted to particles having velocity v_G , and α_{v_G} is an independent constant for each value of v_G .

Now equation (53), for an infinite number of values of v_G could be represented on figure 7 by an infinite number of parallel straight lines, at different levels determined by the values of α_{v_G} . Clearly, the relative values of α_{v_G} , and hence the relative

levels of the straight lines at any value of m , would represent the distribution of v_G .

Then, if the masses were converted from m_∞ to m'_∞ , each straight line in figure 7 would still represent the cumulative mass distribution for the pertinent velocity v_G , but it would be shifted from left to right, or the reverse, because of the change of the mass scale in multiplying by a power of v_∞ . But after all the straight lines were shifted horizontally, the same effect would exist as if they had been shifted vertically. That is, the effect would simply be to change all the values of α_{v_G} in equation (53), thus changing the distribution of v_G but leaving it still the same for one value of m_∞ as for another, or the same for one value of m'_∞ as for another.

Although the author does not now believe appendix F of reference 2 proves the linear relation of luminous efficiency and meteor velocity, he believes this relation, or possibly a linear relation to a power of v_∞ other than unity, is much more plausible than equation (50) with the function $\epsilon(m_\infty, v_\infty)$ conforming to Öpik's formulation in reference 15, as will now be explained by a train of logic involving both the results of the present study and the correlations presented by Dalton in reference 14.

In review of the combined theoretical and empirical derivation of equation (45) of reference 1, it may be seen that such equation, for relative rather than absolute values, is approximately equivalent to

$$C_{\text{marg}} = m_c \tau_c v_\infty^{1.93} \quad (55)$$

where m_c is the true mass and τ_c is the true luminous efficiency on a photographic basis. In converting to equation (55), for simplicity, the exponent of m_∞ has been equated to one. Also the powers of $\cos Z_R$ and $F(Z_R)_{\text{min}}$, which would have cancelled later in this treatment, have been dropped. We may also write

$$m_c \tau_c \propto m_\infty v_\infty \quad (56)$$

because m_∞ was obtained by dividing $m_c \tau_c$ by a constant and by v_∞ . From the right-hand side of proportionality (56), it is clear that according to the results of the present study the product $m_c \tau_c$ is statistically independent of v_∞ .

Now equation (55) is an expression regarding marginal effective exposure. By comparing equations (39), (40), and (45) of reference 1, one may see that equation (55) becomes simply an expression for maximum effective exposure of any meteor upon multiplication of the right-hand side by the constant k_5 of reference 1. Thus,

$$E_{\text{eff(max)}} = k_5 m_c \tau_c v_\infty^{1.93} \quad (57)$$

Equation (57) may be converted to a kind of magnitude related to conditions on the photographic plate as

$$M_{\text{exp}} = M_0 - 2.5 \log m_c - 2.5 \log \tau_c - 4.82 \log v_\infty \quad (58)$$

where M_0 is a constant that need not be evaluated.

If values of M_{exp} according to equation (58) are adjusted to values $M_{\text{exp}(11)}$ that would have existed if the same meteor had had a velocity $v_\infty = 11$ kilometers per second, and if meteors are then ranked in ascending values of $M_{\text{exp}(11)}$, as Dalton has done with equation (15) of reference 14, the meteors should thereby be ranked in descending order of both maximum effective exposure and mass m_c , because m_c would be the only variable that could affect the exposure. Then, if a limited number of the top ranking meteors are taken as a subsample, no weighting factor would be needed to correct mass and velocity biases because no particles within the mass range of the subsample could fail to be discovered.

The adjustment to 11 kilometers per second should change equation (58) to

$$M_{\text{exp}(11)} = M_0 - 2.5 \log m_c - 2.5 \log \tau_{c(11)} - 4.82 \log 11 \quad (59)$$

where $\tau_{c(11)}$ is the true value of luminous efficiency that should exist for the same mass m_c at the velocity $v_\infty = 11$ kilometers per second. By equations (58) and (59),

$$M_{\text{exp}(11)} = M_{\text{exp}} + 2.5 \log \left[\frac{\tau_c}{\tau_{c(11)}} \right] + 4.82 \log \left(\frac{v_\infty}{11} \right) \quad (60)$$

Equation (42) of reference 1 provides a value of an adjusted magnitude M_{adj} in terms of the values of photographic magnitude M_{pg} reported in reference 10. With the simplifying approximation that the meteor height for maximum effective exposure is always the same, and neglecting the resulting constant term, that equation reads

$$M_{\text{adj}} = M_{\text{pg}} + 2.5 \log v_\infty \quad (61)$$

The value of M_{adj} of equation (61) should relate to the maximum effective exposure of equation (57) multiplied by some constant, which for present purposes may be ignored. Hence, by equations (60) and (61),

$$M_{\text{exp}(11)} = M_{\text{pg}} + 2.5 \log \left[\frac{\tau_c}{\tau_{c(11)}} \right] + 7.32 \log \left(\frac{v_\infty}{11} \right) + 2.5 \log(11) \quad (62)$$

For the purpose of ranking meteors in ascending order of $M_{\text{exp}(11)}$, the constant term may be ignored, resulting in

$$M_{\text{exp}(11)} = M_{\text{pg}} + 2.5 \log \left[\frac{\tau_c}{\tau_c(11)} \right] + 7.32 \log \left(\frac{v_\infty}{11} \right) \quad (63)$$

Equation (63) does not differ greatly from Dalton's equation (15). This author agrees with Dalton, therefore, that his equation (15), with a correct formulation for luminous efficiency, should rank meteors approximately in descending order of both maximum effective exposure and particle mass. The neglected effects of zenith angle and position of meteor in field of view were presumably accounted for by the authors of reference 10 in their determination of M_{pg} . Also, if an incorrect formulation for τ_L is used instead of τ_c , equation (63) should rank the meteors in descending order of the incorrect masses determined with the incorrect values of τ_L , and in the order of the incorrect values of maximum effective exposure determined on the same basis.

Now let it be assumed, as in this study, that correctly $k = 1$ and $\epsilon(m_\infty, v_\infty) = 1$ in equation (50). It follows then that Dalton's equation (15) and equation (63) of this report are identical in effect if his equation (15) is used with the correct value $k = 1$ and equation (63) is used with $k = 0.57$. So, for his sample A, he has in effect used equation (63) with $k = 0.57$. Meteors would be ranked in the order $m_\infty v_\infty^{1-k}$, or $m_\infty v_\infty^{0.43}$. Selection of the 333 highest ranking meteors would therefore be improperly biased in favor of high velocity meteors. But this bias should militate against observational failure. In fact, as pointed out earlier, if $k = -1.93$ the entire sample of sporadic meteors reported in reference 10 can be used without any effect of observational failure.

But the product $m_\infty v_\infty^{1-k}$ has been shown to be statistically independent of v_∞ . Hence, with $k = 0.43$ and $\epsilon(m_\infty, v_\infty) = 1$ and with even less observational failure than with $k = 1$, no correlation of mass and velocity might occur, even though the results shown in column two of table II indicate that the subsample of 333 meteors used by Dalton is too large to avoid appreciable observational failure. Contrariwise, if k were given a value greater than unity for use in equation (63) observational failure would be increased. The failure would improperly exclude from the subsample meteors having both low velocity and low mass. A consequent negative linear correlation of the product $m_\infty v_\infty^{1-k}$ with v_∞ should result.

As has been shown in the present study, and partially confirmed by Dalton, the product $m_c \tau_c$ (see eq. (56)) is statistically independent of velocity v_∞ . It is possible (very remotely) that the product of m_c and τ_c could be statistically independent of v_∞ while either one alone correlates linearly with v_∞ . But this possibility appears to be exceedingly unlikely, particularly in view of these facts: (1) if m_c correlates with velocity v_∞ , it must do so because of different mass distributions for different heliocen-

tric orbits with no relation whatever to meteor physics in Earth's atmosphere; and (2) if τ_c correlates with velocity v_∞ , the reasons are associated solely with meteor physics in Earth's atmosphere, with no relation whatever to heliocentric orbits of the particles. Yet, if the product $m_c \tau_c$ is statistically independent of v_∞ , while m_c correlates linearly with v_∞ , the correlations of m_c and τ_c with v_∞ must cancel for all heliocentric orbits. The improbability of such a condition seems to be enormous.

In an analysis like Dalton's, if k of equation (50) were given too great a value in relation to the size of his subsample, a false negative correlation should occur. But no such effect, either positive or negative, could be produced by making k too small. It appears that the present study can throw no light on the proper value of k , even with the help of Dalton's analysis.

However, it is believed that this study, in conjunction with Dalton's results, indicates a great implausibility that $\epsilon(m_\infty, v_\infty)$ should substantially change the velocity dependence of τ_L for different values of m_∞ . If it did so, the reasoning described in equations (53) and (54) and the textual material immediately following those equations would not apply. The effect of the changed formulation for τ_L would not merely shift the infinite number of hypothetical straight lines in figure 7 from side to side without change in slope or shape. The lines would be changed in shape, slope, or both. These changes could not generally be equivalent to vertical shifts without change of shape or slope. Consequently, the distribution of velocity v_∞ would become different for different values of m_∞ . A linear correlation between m_∞ and v_∞ would almost certainly be created.

It is in this context, in this author's opinion, that Dalton's correlations have great value. With use of the equivalent of equation (50), with values of k and $\epsilon(m_\infty, v_\infty)$ as implied by Opik in reference 15, he has found a significant positive correlation between mass and velocity v_∞ (see the correlation in his fig. 16 between his m_B and the air-entry velocity for his subsample B, below the diagonal, equal to 0.221. According to the foregoing reasoning, this correlation could only have been caused by the effect of $\epsilon(m_\infty, v_\infty)$, and the correctness of that function in any form that would be represented by Opik's formulation in reference 15 therefore appears to be highly implausible.

Now, recalling the infinity of hypothetical parallel straight lines in figure 7, representing the cumulative mass distributions for an infinity of velocities v_G , consider the nature of the components of equation (50) that would still permit those lines to superimpose on each other by vertical shifting. As has already been shown, such superimposing would be possible for any value of k with $\epsilon(m_\infty, v_\infty) = 1$. But superimposing of the hypothetical lines representing cumulative mass distribution for the infinity of values of v_G , by vertical shifting of the lines, would also be possible under each of the following conditions: (1) with $\epsilon(m_\infty, v_\infty) = 1$ and the factor v_∞^k replaced by any function of v_∞ alone; (2) with $\epsilon(m_\infty, v_\infty)$ a function of m_∞ alone and $k = 0$; and (3) with the factor

v_∞^k replaced by any function of v_∞ and $\epsilon(m_\infty, k_\infty)$ equal to any power of m_∞ , because then the function $\epsilon(m_\infty, v_\infty)$ would merely change the slopes of all the straight lines to the same extent, and even after they were shifted from side to side by the function of v_∞ as a factor they could still be superimposed by vertical shifting.

The results reported here and in references 1 and 2 would not be seriously affected by any later demonstration that any of these conditions are actually true, instead of $k = 1$ and $\epsilon(m_\infty, v_\infty) = 1$. So long as the hypothetical lines in figure 7 could be superimposed by vertical shifting, the true mass and velocity would still be statistically independent. The masses used in reference 10 would still be statistically independent of velocity, and would still be values of a good statistical parameter. The results could be readily converted to another mass scale. In most practical cases conversion of the results to another mass scale would not even be required. The principal expected utility of these results will be in conjunction with expressions for critical damage to components of a spacecraft in terms of true mass and velocity. So long as the true mass and the mass of reference 10 are both independent of velocity, the true mass may be expressed as a function of the mass of reference 10 and velocity v_∞ in any damage criterion that may have been derived in terms of the true mass, and the damage criterion could then be used in conjunction with the results of this study without any modification.

CONCLUDING REMARKS

The results of this analysis strengthen and refine the conclusions reached in references 1 and 2. As a result, certain assumptions that were made in derivation of the weighting factor for correction of mass and velocity biases in reference 1 may now be virtually removed from the category of assumptions. The exponent of v_∞ in the weighting factor is now more precisely and more firmly determined.

The value of $\beta = 1.34$ in the equation for cumulative mass distribution is no longer an assumption, or even an extrapolation, throughout the mass range of photographic meteors.

The question of a single velocity distribution for all masses is now in the same status as the value of β . It was introduced as an assumption in reference 1 at about the same point as the first use of equation (36) with β equal to 1.34. The derivation of the value of C_{marg} did not depend upon it; the derivation of φ_w did. But the successful duplication of the trends of the data for observed distributions of v_G for all mass groups, with use of the same equation (41) for all, is a direct indication of the same distribution of v_G for all masses. Apparently the only possibility of a false indication here is a hypothetical error in assuming a normal distribution curve governing the fail-

ure to discover meteor traces of near marginal densities. The error in that assumption would have to be of a very specific nature, such that it would create a false fit to the velocity data in figure 5. As the values of μ_d and σ_d that were used affected only the leftward region in each of the curves in figure 5, such a contingency does not seem reasonable.

The determination of the value of $\alpha = 10^{-14.525}$ in equation (36) by use of the level of the plotted points in figure 7 is believed to be superior to the determination of the value $10^{-14.63}$ in reference 2.

A firm velocity distribution has been derived (eq. (41)), in an integrable form. It is believed the distribution represented by this equation already has support independently of the work performed by this author, because it apparently would fit almost exactly the velocity distribution shown by Erickson (ref. 16) if his distribution were converted from v_∞ to v_G . This equation should be understood as defining only the statistically expected velocity distribution upon a surface having random orientation and traveling in the orbit of Earth, but at a sufficiently great distance from Earth that Earth's gravitation has negligible influence on meteoroid velocity. It should also be understood that this equation, like all the results of reference 2 and the present analysis, are without any correction for spacewise bias. That is, as meteoroids impacting the Earth from different directions in space have differing probabilities of impact upon the atmosphere over the camera sites in New Mexico, as well as differing average impact velocities, neglect of those facts should be expected to cause at least a small error in the velocity distributions reported here and in reference 2.

The substantial segment of meteor theory (refs. 3 to 9) that was used in derivation of the weighting factor in reference 1, and hence used in obtaining the theoretical results reported in reference 2, is now supported by the agreement between those theoretical results and the empirical results of the present study.

Lewis Research Center,
National Aeronautics and Space Administration,
Cleveland, Ohio, January 14, 1970,
721-03.

APPENDIX A

SYMBOLS

A_r	area under a curve representing normalized velocity distribution, but reduced by observational failure, nondimensional
a	coefficient of a power of e in normal or log-normal distribution equation, normalized to produce total area under distribution curve equal to probability that random variable will exist within the regime governed by the equation, nondimensional
a'	(with or without subscript) coefficient of a power of e in normal or log-normal distribution equation, normalized to produce unity area under distribution curve
C_{marg}	criterion for marginal photographic density, which, at a critical value, approximately marks the difference between possibility and no possibility for finding trace of meteor on photographic plate, unspecified unit
C_1	constant defined by equation (23), unspecified unit
D	photographic density, that is, logarithm to base 10 of a ratio equal to a quantity of light incident upon a photographic emulsion divided by the quantity of that light transmitted by the emulsion, nondimensional
D_d	photographic density at which an individual meteor trace will be discovered under hypothetical condition of gradual increase of density during observation, nondimensional
D_x	arbitrarily specified value of photographic density, nondimensional
D_0	theoretical density for unity value of exposure, nondimensional
E	exposure, or integrated product of light intensity incident upon a photographic plate and the differential time throughout which the plate is exposed to that light, unspecified unit
$E_{\text{eff(max)}}$	maximum effective exposure produced by meteor on photographic plate (eq. (57))
$F(D_x)$	(unsubscripted) theoretical fraction of meteor traces discovered with a given photographic density D_x
$F(D_x)_j$	theoretical fraction of meteor traces discovered within a subrange of mass j for a value of D_x corresponding to the median mass of the subrange j and corresponding to a given value of unaccelerated velocity v_{G_x}

F_i	($i = 1$ to $i = 10$) fraction of meteoroids within mass group i , of all velocities, that are discovered on photographic plates
$F_i(v_G)$	($i = 1$ to $i = 10$) fraction of meteoroids within mass group i , for velocity v_G alone, that are discovered on photographic plates
$F_{>m}$	influx rate of meteors of mass greater than m , $m^{-2} \text{sec}^{-1}$
$F(Z_R)$	function of Z_R , azimuth of meteor path, and position of meteor within field of view of cameras as defined in reference 2, nondimensional
$F(Z_R)_{av}$	average value of $F(Z_R)$ calculated for each meteor as part of the effort reported in reference 2, nondimensional
$f()$	(with or without subscript, with the blank between parentheses replaced by any variable, such as w) statistical frequency of w , that is, the reciprocal of dw multiplied by the fraction of total cases in which the parameter measured as w has the value $w \pm \frac{1}{2} dw$, nondimensional
$f(v_G)_{ri}$	statistical frequency of v_G , for mass group i , reduced by failure of observation, and not normalized after reduction, nondimensional
k	exponent of v_∞ in expression for luminous efficiency of meteor (eq. (50))
k_5	constant from ref. 1, value unneeded
M_{adj}	adjusted photographic magnitude of meteor related to value M_{pg} from ref. 10 by eq. (61)
M_{exp}	magnitude of meteor as referred to its uncorrected effective exposure on photographic plate
$M_{exp(11)}$	value of M_{exp} corrected to velocity of 11 km/sec
M_{pg}	photographic magnitude of meteor as given in ref. 10
M_0	constant as defined for eq. (58)
m	(without subscript) arbitrarily specified value of m_∞
m	(with subscript other than ∞) value of m_∞ for conditions defined by the subscript, g
m_c	hypothetical correct value of m_∞ unrelated to manner of evaluation
m_∞	mass of a meteoroid before any ablation by Earth's atmosphere, g (always understood to represent value shown in ref. 10 unless otherwise specified)
n	number of subranges of value of mass m_∞ used in fitting bimodal log-normal distribution equation to data for values of velocity v_G for different mass groups

$p \{ \}$	probability of occurrence of condition expressed within braces
$p \{ E_x \}$	(with or without subscript) probability of existence of random variable or probability that random variable if it exists will lie within a specified regime
R	in a bimodal log-normal distribution equation, ratio of incidence attributable to second mode to that attributable to first mode, as in eq. (16)
t	variable of integration, which, in any definite integral, represents the variable for which specific values are used as the limits of integration
v_e	velocity of escape from Earth's gravity, km/sec
v_G	velocity of a meteoroid relative to Earth at time of impact as it would have existed if not accelerated by Earth's gravity, km/sec
v_∞	velocity of a meteoroid relative to Earth's atmosphere after full acceleration by Earth's gravity but before any deceleration by atmospheric friction, km/sec
Z	natural logarithm of z
Z_R	angle of a meteor path to the zenith within Earth's atmosphere, deg
z	in the expression for a single mode in a log-normal distribution equation, the argument of the mean logarithm μ ($v_G + \delta$ in eq. (11))
α	a constant in eq. (36) for mass influx rate of meteors, equal to $10^{-14.525}$ or 2.98×10^{-15} as indicated by the lower straight-line graph in fig. 7, $g^\beta m^{-2} \text{sec}^{-1}$
β	negative value of the exponent of m in equation (36) for mass rate of influx of meteoroids
γ	slope of a graph representing the density of darkening of a photographic emulsion relative to the logarithm to the base 10 of the exposure that caused the darkening, unspecified units
δ	(with or without subscript) in the expression for a single mode, in a log-normal distribution equation such as (11), the offset of the exponential of the mean logarithm μ from the modal value of the random variable
$\epsilon(m_\infty, v_\infty)$	function of m_∞ and v_∞ used in equation (50), containing no constant non-zero power of v_∞ as a factor independently of m_∞
μ	(without subscript) mean value of the argument w in the frequency function $f(w)$ in an ordinary normal distribution equation for a single mode, or the mean logarithm occupying an analogous position in a log-normal equation, like 2.46 (ln 11.7) in eq. (47)

μ	(with subscript 1 or 2) like unsubscripted μ , but for mode 1 or 2 of a bimodal equation
μ_d	density of meteor trace on photographic plate at which one-half of traces are discovered by observers, nondimensional
ν	exponent of mass m_∞ in a hypothetical expression for weighting factor φ_w
ξ	exponent of velocity v_∞ in a hypothetical expression for weighting factor φ_w
σ	(without subscript or with subscript 1 or 2) standard deviation measured from the value μ (unsubscripted or with subscript 1 or 2) in a normal distribution equation, or occupying analogous position in a log-normal equation, like 0.44 in eq. (47)
σ_d	standard deviation of density on photographic plates at which observers fail to discover meteor traces, measured from the density μ_d , nondimensional
σ'_h	an arbitrarily defined approximation of standard deviation, for use on the high side only of the mean value in a Poisson distribution, within which approximately 68 percent of values of the random variable on the high side of the mean should be found
τ	in a normal distribution, the difference, measured as a multiple of the standard deviation σ , between the argument w of the frequency function $f(w)$ and the mean value of w
τ_0	value of luminous efficiency τ_L that would exist at velocity $v_\infty = 1$ km/sec and $\epsilon(m_\infty, v_\infty) = 1$ (eq. (50))
τ_c	hypothetical correct value of τ_L
$\tau_{c(11)}$	value of τ_c for given meteor corrected to 11 km/sec
τ_L	luminous efficiency of a meteor on a photographic basis, or fraction of dissipated kinetic energy that is converted to actinic value at photographic plate
τ_x	an arbitrarily specified value of τ
$\varphi(x)$	probability that a random variable conforming to the Poisson distribution will have the arbitrarily specified integral value x
φ_w	weighting factor for simultaneous correction of velocity and mass biases involved in photography of meteors, nondimensional

APPENDIX B

NORMALIZING FACTOR FOR OFFSET LOG-NORMAL DISTRIBUTION

With an assumption of certainty that the velocity v_G will be within a regime governed by equation (11), the constant a' in that equation is expressible as a function that will now be derived in terms of μ and σ as they appear in the same equation.

The problem is to provide a total probability equal to unity that the random variable will have some value or other. That is, $f(v_G)$ in equation (11) must satisfy the requirement that

$$\int_0^\infty f(v_G) dv_G = 1 \quad (B1)$$

The problem may be simplified if $-\delta$ may be substituted for the lower limit of the integral in equation (B1). If δ is negative or zero, such substitution may be made because $f(v_G)$ by equation (11) will then be either zero or imaginary for positive values of v_G less than the numerical value of δ , which will mean that any such value of v_G is outside the regime governed by equation (11). The substitution may also be made for practical purposes if δ is positive and is interrelated with μ and σ in such a manner that the integral of $f(v_G) dv_G$ between $v_G = -\delta$ and $v_G = 0$ is negligibly small. Such a case is equation (47), although that fact is academic because the coefficient 0.070 was found in reference 2 empirically.

Now, to determine a proper value of a' , substitutions will be made as follows:

$$z = v_G + \delta \quad (B2)$$

and

$$Z = \ln z \quad (B3)$$

Now equation (11) will be rewritten as

$$f(v_G) = a' \exp \left[-\frac{1}{2} \left(\frac{\ln z - \mu}{\sigma} \right)^2 \right] \quad (B4)$$

By statistical theory (see ref. 11 or other text on mathematical statistics),

$$f(Z) = f(v_G) \frac{dv_G}{dZ} \quad (B5)$$

From equations (B4) and (B5),

$$\left. \begin{aligned} f(Z) &= a' \exp \left[-\frac{1}{2} \left(\frac{\ln z - \mu}{\sigma} \right)^2 \right] \frac{d}{dz} (z - \delta) \\ &= a' e^Z \exp \left[-\frac{1}{2} \left(\frac{Z - \mu}{\sigma} \right)^2 \right] \end{aligned} \right\} \quad (B6)$$

The squared binomial in the second exponential may be expanded, terms of both exponentials in Z may be combined, and a new squared binomial may be formed incorporating all terms in Z or Z^2 , with the result

$$f(Z) = a' \exp \left(\mu + \frac{1}{2} \sigma^2 \right) \exp \left\{ -\frac{1}{2} \left[\frac{Z - (\mu + \sigma^2)}{\sigma} \right]^2 \right\} \quad (B7)$$

Equation (B7) is an ordinary normal distribution of Z . Hence, equation (B1), with the substitution of $-\delta$ for the lower limit of integration, must apply in the form

$$\int_{-\infty}^{\infty} a' \exp \left(\mu + \frac{1}{2} \sigma^2 \right) \exp \left\{ -\frac{1}{2} \left[\frac{Z - (\mu + \sigma^2)}{\sigma} \right]^2 \right\} dZ = 1 \quad (B8)$$

So, from equations (3) and (B8), since a' of equation (3) for a normal distribution corresponds to the total coefficient $a' \exp \left(\mu + \frac{1}{2} \sigma^2 \right)$ in equation (B7),

$$a' \exp \left(\mu + \frac{1}{2} \sigma^2 \right) = \frac{1}{\sqrt{2\pi} \sigma} \quad (B9)$$

which is the same as equation (12).

APPENDIX C

STATISTICAL EFFECT OF ZENITH ANGLE AND POSITION OF METEOR WITHIN FIELD OF VIEW

Equation (20) was derived on an empirical basis in reference 1. It was used there and in reference 2, with other considerations, for development of the weighting factor

$$\varphi_w = (\cos Z_R)^{-0.196} F(Z_R)_{av}^{0.730} v_\infty^{-4.22} \left[1 + \left(\frac{v_e}{v_G} \right)^2 \right]^{-1} \quad (C1)$$

Without the bracketed expression, the correction for gravitational focusing, equation (C1) would be the same as equation (75) in reference 1.

In a computer run described in reference 2, this weighting factor was applied to the data for 2021 sporadic meteors reported in reference 10, to obtain a corrected histogram (ref. 2 (fig. 1(b))) for unaccelerated meteoroid velocities. A histogram for the unaccelerated velocities has also been obtained with the same weighting factor, but with omission of $(\cos Z_R)^{-0.196}$ and $F(Z_R)_{av}^{0.730}$, that is, with the following factor,

$$\varphi_w = v_\infty^{-4.22} \left[1 + \left(\frac{v_e}{v_G} \right)^2 \right]^{-1} \quad (C2)$$

Both histograms are shown in figure 9, the circular symbols representing the results with equation (C1), the square points with equation (C2).

The cameras used for obtaining the data reported in reference 10 were operated at all feasible hours of the night, and on dates nearly uniformly distributed throughout the year. For that reason, the effects of $\cos Z_R$ and $F(Z_R)_{av}$ might well be expected to be nearly or entirely nullified statistically. The trends of the two results as shown in figure 9 are only slightly different. Hence, the statistical nullification, or averaging out, of the effects of $\cos Z_R$ and $F(Z_R)_{av}$ for so large a sample is approximately confirmed.

This result does not obviously justify omission of the factors $(\cos Z_R)^{0.167}$ and $F(Z_R)_{av}^{-0.54}$ in equation (20) to yield equation (21). However, the purpose in the use of equation (21) in the present paper is to obtain an empirical end result comparable with the theoretical end result obtained with equation (C1) in reference 2. Hence, it is believed the comparison in figure 9 justifies the transition from equation (20) to (21).

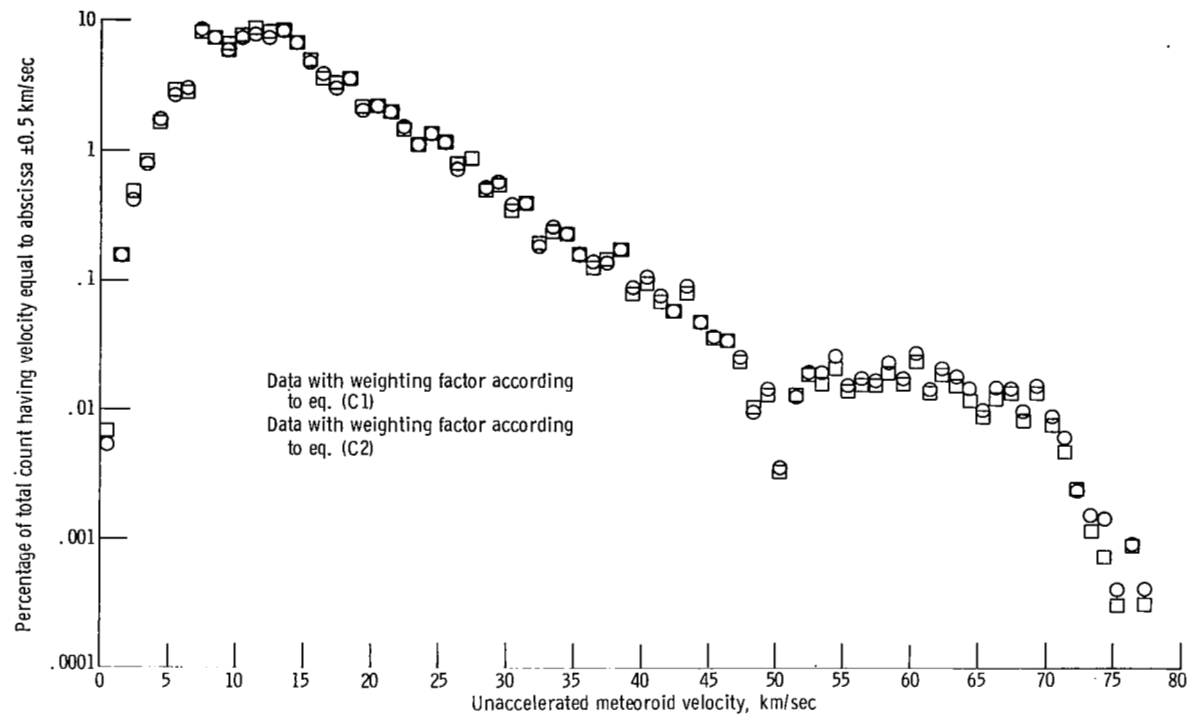


Figure 9. - Velocity distribution of sporadic meteors relative to gravity-free Earth weighted as velocity relative to atmosphere to -4.22 power.

APPENDIX D

ERRORS IN EARLIER PUBLICATION ON ANALYSIS OF METEOR DATA

The author now believes that certain statements on pages 55 to 57 of reference 2 were not justified, as follows:

(1) On page 55, fifth line following equation (F14), the "theoretically correct expression for φ_w " would be so only as applied with a given lower limit of m_∞ (even if the values of m'_∞ were correct).

(2) On page 55, 11th and 12th lines below equation (F14), the statement " φ_w (1) is a correct weighting factor" also applies only with a given lower limit of m_∞ .

(3) The sentence beginning in the third line after equation (F22) on page 57 is not believed to be correct. The weighting factor was confirmed for any given lower limit of m_∞ (even for n not equal zero). It is now believed a correct weighting factor could have been found with use of equation (F22), for application with a given lower limit value of m'_∞ . With similar reasoning, it is now believed the last four lines of the next to last paragraph and the entire last paragraph on page 57 are not correct.

With the exceptions noted, the author still regards all of appendix F of reference 2 as valid.

REFERENCES

1. Miller, C. D.: Simultaneous Correction of Velocity and Mass Bias in Photography of Meteors. NASA TR R-280, 1968.
2. Miller, C. D.: Unaccelerated Geocentric Velocities and Influx Rates of Sporadic Photographic Meteors. NASA TN D-5245, 1969.
3. Whipple, Fred L.: On Meteoroids and Penetration. Smithsonian Astrophysical Observatory, 1963.
4. Hawkins, Gerald S.; and Upton, Edward K. L.: The Influx Rate of Meteors in the Earth's Atmosphere. *Astrophys. J.*, vol. 128, no. 3, Nov. 1958, pp. 727-735.
5. Öpik, Ernst: Atomic Collisions and Radiation of Meteors. Rep. 100, Harvard College Observatory, 1933.
6. Jacchia, Luigi G.: The Physical Theory of Meteors. VIII. Fragmentation as Cause of the Faint-Meteor Anomaly. *Astrophys. J.*, vol. 121, no. 2, Mar. 1955, pp. 521-527.
7. Jacchia, Luigi G.: On Two Parameters Used in the Physical Theory of Meteors. *Smithsonian Contributions to Astrophysics*, vol. 2, no. 9, 1958, pp. 181-187.
8. Hawkins, Gerald S.; and Southworth, Richard B.: The Statistics of Meteors in the Earth's Atmosphere. *Smithsonian Contributions to Astrophysics*, vol. 2, no. 11, 1958, pp. 349-364.
9. Verniani, Franco: On the Luminous Efficiency of Meteors. Special Rep. No. 145, Smithsonian Astrophysical Observatory (NASA CR-55904), Feb. 17, 1964.
10. McCrosky, Richard E.; and Posen, Annette: Orbital Elements of Photographic Meteors. *Smithsonian Contributions to Astrophysics*, vol. 4, no. 2, 1961, pp. 15-84.
11. Hoel, Paul G.: *Introduction to Mathematical Statistics*. Third ed., John Wiley & Sons, Inc., 1962.
12. Dwight, Herbert B.: *Tables of Integrals and Other Mathematical Data*. Fourth ed., Macmillan Co., 1961.
13. Henney, Keith; and Dudley, Beverly, eds.: *Handbook of Photography*. McGraw-Hill Book Co., Inc., 1939.
14. Dalton, Charles C.: Determination of Meteoroid Environments from Photographic Meteor Data. NASA TR R-322, 1969.
15. Öpik, Ernst J.: *Physics of Meteor Flight in the Atmosphere*. Interscience Publ., Inc., 1958.

16. Erickson, James E.: Velocity Distribution of Sporadic Photographic Meteors.
J. Geophys. Res., vol. 73, no. 12, June 15, 1968, pp. 3721-3726.

NATIONAL AERONAUTICS AND SPACE ADMINISTRATION

WASHINGTON, D. C. 20546

OFFICIAL BUSINESS

FIRST CLASS MAIL



POSTAGE AND FEES PAID
NATIONAL AERONAUTICS AND
SPACE ADMINISTRATION

POSTAGE AND FEES PAID
NATIONAL AERONAUTICS AND SPACE ADMINISTRATION
SPECIAL DELIVERY MAIL

POSTAGE AND FEES PAID
NATIONAL AERONAUTICS AND SPACE ADMINISTRATION

POSTMASTER: If Undeliverable (Section 158
Postal Manual) Do Not Return

"The aeronautical and space activities of the United States shall be conducted so as to contribute . . . to the expansion of human knowledge of phenomena in the atmosphere and space. The Administration shall provide for the widest practicable and appropriate dissemination of information concerning its activities and the results thereof."

— NATIONAL AERONAUTICS AND SPACE ACT OF 1958

NASA SCIENTIFIC AND TECHNICAL PUBLICATIONS

TECHNICAL REPORTS: Scientific and technical information considered important, complete, and a lasting contribution to existing knowledge.

TECHNICAL NOTES: Information less broad in scope but nevertheless of importance as a contribution to existing knowledge.

TECHNICAL MEMORANDUMS: Information receiving limited distribution because of preliminary data, security classification, or other reasons.

CONTRACTOR REPORTS: Scientific and technical information generated under a NASA contract or grant and considered an important contribution to existing knowledge.

TECHNICAL TRANSLATIONS: Information published in a foreign language considered to merit NASA distribution in English.

SPECIAL PUBLICATIONS: Information derived from or of value to NASA activities. Publications include conference proceedings, monographs, data compilations, handbooks, sourcebooks, and special bibliographies.

TECHNOLOGY UTILIZATION PUBLICATIONS: Information on technology used by NASA that may be of particular interest in commercial and other non-aerospace applications. Publications include Tech Briefs, Technology Utilization Reports and Notes, and Technology Surveys.

Details on the availability of these publications may be obtained from:

SCIENTIFIC AND TECHNICAL INFORMATION DIVISION

NATIONAL AERONAUTICS AND SPACE ADMINISTRATION

Washington, D.C. 20546